A Simulation-Based Optimization Algorithm for Dynamic Large-Scale Urban Transportation Problems

A simulation-based optimization algorithm for dynamic large-scale urban transportation problems

Linsen Chong, Carolina Osorio
Civil and Environmental Engineering Department, Massachusetts Institute of Technology, Office 1-232, Cambridge, Massachusetts 02139, USA, linsenc@mit.edu, osorioc@mit.edu,

This paper addresses large-scale urban transportation optimization problems with time-dependent continuous decision variables, a stochastic simulation-based objective function, and general analytical differentiable constraints. We propose a metamodel approach to address, in a computationally efficient way, these large-scale dynamic simulation-based optimization problems. We formulate an analytical dynamic network model that is used as part of the metamodel. The network model formulation combines ideas from transient queueing theory and traffic flow theory. The model is formulated as a system of equations. The model complexity is linear in the number of road links and is independent of the link space capacities. This makes it a scalable model suitable for the analysis of large-scale problems.

The proposed dynamic metamodel approach is used to address a time-dependent large-scale traffic signal control problem for the city of Lausanne. Its performance is compared to that of a stationary metamodel approach. The proposed approach outperforms the stationary approach. This comparison illustrates the added value of providing the algorithm with analytical dynamic problem-specific structural information. The performance of a signal plan derived by the proposed approach is also compared to that of an existing signal plan for the city of Lausanne and to that of a signal plan derived by a mainstream commercial signal control software. The proposed method can systematically identify signal plans with good performance.

Key words: simulation-based optimization, transient queueing theory, metamodel

1. Introduction

In the field of urban transportation, dynamic optimization problems, i.e., optimization problems with time-dependent decision variables, have been addressed through the use of analytical dynamic and, mostly deterministic, traffic models. Such models are based on an aggregate, i.e., low-resolution, description of traffic dynamics. They are computationally efficient to evaluate, yet lack a detailed description of heterogeneous traveler behavior, of vehicle-infrastructure interactions, and thus of intricate traffic dynamics observed in urban areas. A detailed description of these dynamics is provided by a family of high-resolution simulation-based traffic models, known as stochastic microscopic or mesoscopic traffic simulators. Nonetheless, these simulators are computationally inefficient to evaluate. Hence, their use to address optimization problems has been limited. This paper proposes a methodology that enables high-resolution traffic simulators to be used, in a computationally efficient way, to address large-scale dynamic transportation optimization problems.

The complexity of the spatial-temporal vehicle-to-vehicle and vehicle-to-infrastructure interactions has lead to the development of these high-resolution simulation-based traffic models. These simulators emulate the behavior of individual travelers, e.g., how they make pre-trip travel decisions (e.g., departure-time, travel mode, travel route) and en-route travel decisions (e.g., driving behavior). They describe traffic dynamics at the scale of individual, and heterogeneous, vehicles and travelers. Additionally, stochastic microscopic or mesoscopic models can account for uncertainties in both demand and supply components.

Given the increasing complexity of both network supply (e.g., traffic-responsive priority-based traffic control strategies) and network demand (e.g., ubiquitous access and reaction to real-time traffic information by individual travelers), major urban transportation agencies, such as the New York City Department of Transportation (Chen et al. 2015), have resorted to the use of such models to inform their network design and network operations. Nonetheless, this high-resolution description of traffic dynamics comes with a significant increase in the model complexity and the computational cost of evaluating the model. Hence, the use of these high-resolution traffic models for optimization is limited. To the best of our knowledge, they have not been used to address dynamic transportation optimization problems; let alone large-scale dynamic problems.

This paper focuses on optimization problems of the following form:

$$\min_{x_1,\ldots,x_L} f(x,z;p) = \frac{1}{L}\sum_{\ell=1}^{L} E[F_\ell(x_\ell, z_\ell; p)] \tag{1}$$

$$g_\ell(x_\ell; p) = 0 \quad \forall \ell \in \mathcal{L}. \tag{2}$$

The time horizon is decomposed into a set of L disjoint time intervals $\mathcal{L}$. Each time interval ℓ considers a continuous decision vector x_ℓ (e.g., traffic signal plan), an objective function defined as the expectation of a network performance function F_ℓ (e.g., trip travel time, network throughput within interval ℓ). The latter depends on a vector of interval-dependent decision variables x_ℓ and endogenous variables z_ℓ (e.g., link travel times, traffic assignment), and a vector of interval-independent exogenous parameters p (e.g., network topology). The decision vector for all time intervals is denoted $x = (x_1, \ldots, x_L)$, similarly we denote $z = (z_1, \ldots, z_L)$. For time interval ℓ, the feasible region is defined by a set of general analytical and differentiable constraints, g_ℓ. This precludes the use of simulation-based constraints (constraints that need to be evaluated via simulation). This is why the function g_ℓ does not depend on the endogenous simulation variables z_ℓ. A discussion on problems with simulation-based constraints is given in the Conclusions of this paper (Section 5). Note that Constraint (2) is a general formulation for any type of constraint, i.e., inequality constraints can be transformed and expressed as equality constraints of the form (2). To summarize, Problem (1)-(2) considers a time-dependent decision vector with a simulation-based objective function and general, analytical, differentiable constraints. Hereafter, Problem (1)-(2) is referred to as a dynamic simulation-based optimization (SO) problem.

The main challenges of addressing Problem (1)-(2) lie in the objective function, $f(x, z; p)$. The challenges are the following.

- The function f has no known analytical form. We can merely estimate it by running simulation replications of the stochastic traffic simulator.
- An accurate estimation of f is computationally costly to obtain. It involves running numerous simulation replications. In a high-resolution urban traffic simulator, such as the one used in this paper, running a single replication is costly because it involves simulating the travel behavior of typically tens of thousands of individual travelers. The behavior of a single traveler is defined by hundreds of pre-trip and en-route travel decisions (e.g., route choice, lane-changing), which are each simulated by sampling from stochastic travel behavioral models.
- The function f is typically nonconvex. For example, in Section 4 we study a signal control problem where f represents the expected trip travel time of the travelers. In the simulation model, the travel decisions of a given traveler (e.g., route choice) can depend on the state of the network (e.g., congestion patterns), which itself is a consequence of the past decisions of numerous travelers. Hence, the mapping of a signal plan (the decision vector) to network-wide traffic assignment and to the corresponding expected trip travel time (the objective function) is intricate.

This highlights the general complexity of simulation-based problems across all application fields, as well as the additional challenges that are unique to urban transportation problems.

The focus of this paper is to propose computationally efficient algorithms for large-scale dynamic simulation-based problems, i.e., algorithms that can identify solutions with significantly improved objective function values within a tight computational budget (e.g., few simulation runs).

The remainder of this section reviews past work on addressing dynamic SO problems, not limited to transportation applications, followed by a review of SO algorithms for urban transportation problems. We conclude this section by stating the main contributions of this paper.

Dynamic simulation-based optimization problems

The field of supply chain logistics has extensively used detailed stochastic simulators to describe intricate spatial-temporal processes within supply chain networks. Schwartz et al. (2006) and Jung et al. (2004) both consider a dynamic inventory management problem and resort to the use of gradient-based SO algorithms. In both cases, the simulator is seen as a black-box. It is used to obtain objective function and first-order derivative estimates. Nonetheless, no problem-specific analytical structural information is provided to the optimization algorithm. Legato et al. (2008) address a dynamic quay crane scheduling problem at a maritime container terminal. The simulator, a stochastic queueing network model, is also used as a black-box to derive objective function estimates. An approach that addresses a dynamic supply chain problem, and that indeed attempts to exploit problem-specific structure is proposed by Almeder et al. (2009). Although it is not an SO approach, it is worth mentioning because it is also motivated by the ideas of: (i) combining efficient optimization techniques with computationally costly simulation models; and (ii) exploiting problem-specific structural information. In the framework of Almeder et al. (2009): the following two steps are carried out iteratively: (i) certain parameters of the analytical problems (linear programs and mixed-integer programs) are estimated via simulation; (ii) given the estimated parameters, the analytical problems are solved. The iterations are carried out until the distance between consecutive solutions is below a threshold.

To the best of our knowledge, in past work in the field of dynamic SO, the stochastic simulator has been seen as a black-box. It has been coupled with general-purpose algorithms. This allows for flexibility since the proposed frameworks can be readily extended to address a variety of problems. Nonetheless, the proposed methods are not designed to address problems within tight computational budget. In other words, the SO algorithms used are designed to achieve asymptotic performance guarantees rather than good

short-term performance. When using high-resolution computationally expensive simulation models, the simulation run time significantly limits the scale and complexity of the problems that can be addressed. Jung et al. (2004), for instance, clearly state this limitation: "The key limitation of the overall approach lies in the large computing times required to address problems of increasing scope."

Simulation-based optimization for urban transportation problems

The use of high-resolution road traffic simulators for optimization is limited. Rather, they have mostly been used to perform what-if analysis. In other words, they are mostly used to evaluate the performance of a, typically small, set of predetermined alternatives (e.g., traffic management strategies) (Bullock et al. 2004, Ben-Akiva et al. 2003, Hasan et al. 2002, Stallard and Owen 1998, Gartner and Hou 1992, Rathi and Lieberman 1989). Few SO methods that embed high-resolution simulators have been developed (Li et al. 2010, Stevanovic et al. 2008, Branke et al. 2007, Yun and Park 2006, Hale 2005, Joshi et al. 1995). The most common approach is the use of general-purpose heuristic algorithms and, in particular, the use of genetic algorithms (see Yun and Park (2006) for a review). Such algorithms allow to address problems with complex (e.g., nonconvex, simulation-based) objective functions. They are designed such as to achieve suitable asymptotic properties (e.g., convergence properties), rather than to identify points with good performance within few simulation runs. In other words, they are not designed to be computationally efficient. Genetic algorithm case studies for low-dimensional problems report evaluating tens of thousands of points (Kwak et al. 2012, Stevanovic et al. 2009, Park et al. 2009). They are not suitable to address large-scale dynamic problems efficiently.

Paper contributions

This paper proposes an SO algorithm for large-scale networks with high-dimensional time-dependent decision variables, i.e., we propose an SO algorithm for large-scale dynamic transportation problems. The proposed approach is suitable to address a variety of transportation problems that can be formulated as large-scale dynamic continuous simulation-based optimization problems with general analytical constraints.

- We propose a framework to address dynamic SO transportation problems of the form (1)-(2). The framework couples information from the simulator with analytical time-dependent problem-specific structural information. More specifically, a time-dependent analytical traffic model is formulated and used to derive an analytical description of the spatial-temporal congestion patterns observed in the simulator. This analytical information is provided to the SO algorithm. This coupling of information is achieved through

the use of metamodel methods. This combination leads to SO algorithms that are computationally efficient, i.e., they can identify solutions with good performance within few simulation runs.

- To the best of our knowledge, this is the first SO algorithm designed for dynamic problems. It is also the first to enable dynamic transportation SO problems to be addressed in a computationally efficient manner. Efficiency is achieved through the formulation of a tractable transient analytical network model.

- The analytical network model is formulated as a simple system of equations. The model complexity is linear in the number of links in the network and is independent of the link space capacities. This makes it particularly suitable for large-scale networks.

- Our past work has developed efficient SO algorithms for problems with time-independent decision variables. Appendix A summarizes the main methods, results and insights of past work. It serves to motivate the ideas of this paper. The present paper is the first to design an efficient algorithm suitable for SO problems with time-dependent decision variables. In particular, in past work the analytical traffic models used are stationary models. They provide a description of the spatial propagation of congestion, yet do not describe its temporal propagation. The proposed model is a transient model. It describes both the spatial and the temporal propagation of congestion. More specifically, it approximates the temporal variations of the spillback probabilities of each lane. The use of a transient, rather than a stationary, model is recommended for scenarios where congestion varies substantially within each time period (e.g., congestion build-up or dissipation periods). The case study of this paper, indicates that providing the SO algorithm with a temporal description of congestion propagation enables it to identify solutions that delay the onset and the propagation of congestion. The proposed analytical model builds upon the stationary model of Osorio and Chong (2015). A description of their main differences is given in Section 2.4.

- The proposed algorithm is used to address a time-dependent traffic signal control problem. This problem controls the signal plans of 17 intersections distributed across a city with over 600 roads. This is considered large-scale for urban traffic signal control problems (Aboudolas et al. 2010, 2007, Dinopoulou et al. 2006). This problem is a constrained non-convex problem with a decision vector of dimension 198; this is also considered a challenging and large-scale problem in the field of SO. The case study indicates that the proposed method identifies signal plans that outperform: (i) a signal plan prevailing in the field, (ii) a signal plan derived by a commercial signal control software, and (iii) signal plans derived by the SO method of Osorio and Chong (2015), which is designed for time-independent problems.

We present the proposed dynamic SO framework in Section 2. We then apply the framework to address a traffic signal control problem for the city of Lausanne. The optimization problem is formulated in Section 3, the Lausanne city results are presented in Section 4. The main conclusions are presented in Section 5. In our past work, we have developed efficient SO algorithms for various transportation problems with case studies of Lausanne (Switzerland), Manhattan (NYC, USA) and Berlin (Germany). Appendix A summarizes the main insights obtained from past work. The formulation presented in this paper is motivated by these insights. Appendix B details the formulation of the trust region subproblem that is solved at every iteration of the SO algorithm. Appendix C illustrates with an example how the analytical derivatives of the metamodel are derived.

2. Methodology

This paper proposes a new metamodel formulation for SO problems with time-dependent variables. This new formulation is then embedded within the SO algorithm of Osorio and Bierlaire (2013) and used to address a signal control problem. In Section 2.1, we summarize the main ideas of a metamodel SO algorithm. Sections 2.2 and 2.3 describe the proposed model. A summary of the new model is given in Section 2.4.

2.1. Metamodel framework

Metamodel SO algorithms

The main idea of a metamodel SO algorithm is to approximate the unknown simulation-based objective function (Equation (1)) with an analytical function known as the metamodel. The main steps of a metamodel SO algorithm are displayed in Figure 1. At a given iteration k, there are a set of points that have been simulated prior to iteration k. We call these points, and their performance estimates, the current sample. Step 1 determines which point of the current sample is considered to have the best performance. This point is referred to as the *current iterate* and is denoted x_k. In step 2, the parameters, β_k, of the metamodel, m_k, are fitted based on the current sample. For example, in the algorithm used in the case study of this paper, the vector β_k is obtained as the solution of a least squares problem that minimizes the distance, over the current sample, between metamodel values and simulation-based objective function estimates.

Step 3a solves the following problem (or a subproblem of it):

$$\min_{x_1,\dots,x_L} m_k(x, y; q, \beta_k) \tag{3}$$

$$g_\ell(x_\ell; q) = 0 \quad \forall \ell \in \mathcal{L}. \tag{4}$$

This problem differs from Problem (1)-(2) in that the simulation-based objective function f of (1) is replaced with the metamodel function m_k. The latter is an analytical, and

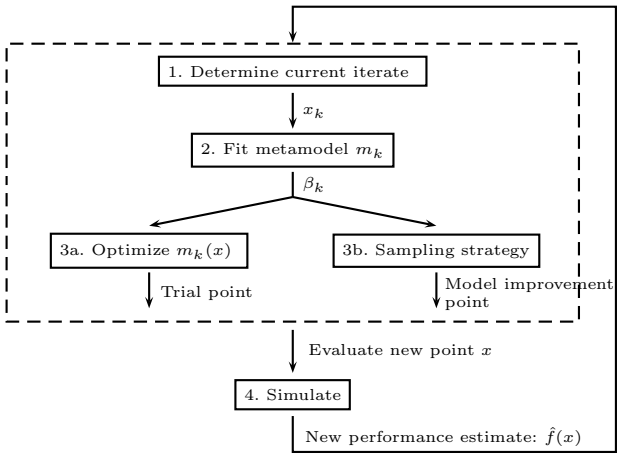

Figure 1 Metamodel simulation-based optimization framework

often differentiable, function that depends on the decision vector $x = (x_1, \ldots, x_L)$, on a vector of endogenous variables $y = (y_1, \ldots, y_L)$, a vector of exogenous parameters, q, and an iteration-specific metamodel parameter vector, β_k. The solution to this problem is called the *trial point*.

Step 3b allows to simulate points that may not be solutions to the approximate problem (3)-(4). These are known as *model improvement points*. The corresponding sampling strategy that defines these points may, for instance, have the goal of improving the properties of the sampled space (e.g., increase the dimension of the space spanned, sample uniformly, etc.) The new points (trial and model improvement) are simulated in step 4 to obtain an estimate of the objective function, denoted $\hat{f}(x)$. As the iterations advance, more points are sampled, leading to an improved metamodel and to points with improved objective function estimates.

One feature of metamodel methods is that the trial points are derived by solving Problem (3)-(4), which is analytical and differentiable. Hence, it can be solved with a variety of mainstream solvers. Additionally, the algorithm we use in this paper (Osorio and Bierlaire 2013) is a derivative-free algorithm. Hence, it does not require the estimation of first- or second-order derivatives of the SO objective function, $f(x)$. Many traditional SO algorithms rely on derivative estimations, which can be computationally costly to obtain in high-dimensional spaces. The use of a derivative-free algorithm is important to achieve computational efficiency.

More generally, SO methods can be classified into three families: (i) direct-search methods, (ii) direct gradient and (iii) metamodel methods. For reviews, see Conn et al. (2009), Balakrishna (2006), Barton and Meckesheimer (2006), Kolda et al. (2003). Direct search methods rely only on simulation-based objective function estimations without fitting an analytical model. Direct gradient methods use estimates of both the objective function

and its derivatives to search the feasible region. To the best of our knowledge, existing direct-search and direct gradient techniques do not perform well for high-dimensional transportation problems and tight computational budgets, see Balakrishna (2006) for a more detailed discussion. As is detailed in Appendix A, metamodel approaches have performed well for such problems.

Metamodel functions

This section describes the main classes of metamodels and their properties. A review of metamodel functions is given in Conn et al. (2009) and in Barton and Meckesheimer (2006). Most metamodel SO work uses general-purpose metamodels (e.g., polynomials). For such models, the functional form of m_k is problem-independent and is typically chosen based on mathematical properties (e.g., tractability). This generality allows the models to be used for a variety of problems, yet it comes at the cost of not capturing problem-specific structure.

Osorio and Bierlaire (2013) proposed the following functional form for the metamodel, at a given iteration k:

$$m_k(x, y; q, \beta_k) = \beta_{k,0} f_A(x, y; q) + \phi(x; \beta_{k,1}, \ldots, \beta_{k,D}). \tag{5}$$

It consists of a linear combination of a problem-specific component (also known as a physical component), denoted f_A, and a general-purpose component, denoted ϕ. The function ϕ is a polynomial that is quadratic in x, and has D coefficients $(\beta_{k,1}, \ldots, \beta_{k,D})$. The problem-specific component f_A is defined as the approximation of f (Equation (1)). It is derived by an analytical macroscopic traffic network model. It is scaled by the scalar coefficient $\beta_{k,0}$. The parameter vector of the metamodel is represented by $\beta_k = (\beta_{k,0}, \ldots, \beta_{k,D})$.

The metamodel m_k can be interpreted as an analytical and macroscopic approximation of the objective function provided by f_A, which is corrected parametrically by both a scaling factor $\beta_{k,0}$ and a separable error term $\phi(x_\ell; \beta_{k,1}, \ldots, \beta_{k,D})$. The general-purpose approximation ϕ also allows to ensure asymptotic algorithmic convergence properties, for more details on this see Osorio and Bierlaire (2013).

The problem solved at a given iteration k of the SO algorithm is of the form:

$$\min_{x_1,\ldots,x_L} m_k(x, y; q, \beta_k) \tag{6}$$

$$g_\ell(x_\ell; q) = 0 \quad \forall \ell \in \mathcal{L} \tag{7}$$

$$h(x, y; q) = 0. \tag{8}$$

This problem differs from Problem (3)-(4) in the Constraint (8). This constraint represents the analytical traffic network model used to derive the physical metamodel component

(i.e., term f_A of Equation (5)). The traffic model used in this paper is a transient network model, that is also analytical and differentiable. It is defined as a system of nonlinear equations and is represented by the function h of Constraint (8).

Problem (6)-(8) is solved at every iteration of the SO algorithm. Therefore, the development of a computationally efficient SO algorithm requires solving Problem (6)-(8) efficiently. Hence, the analytical network model (represented by (8)) needs to be tractable.

The problem-specific approximation f_A contributes to the computational efficiency of the algorithm in various ways. First, as an analytical and differentiable model, it allows for the use of traditional and computationally efficient algorithms (e.g., gradient-based algorithms) to solve Problem (6)-(8). Second, it provides an approximation of f in the entire feasible region, i.e., it provides a global approximation. This is in contrast with traditional general-purpose functions (e.g., polynomial functions) that are designed to provide good local approximations of f. Third, the accuracy of this global approximation is independent of the availability of simulation observations. In particular, if few or even no simulation observations are available, this approximation may still provide a suitable approximation of the objective function f. Fourth, if the network model h (Equation (8)) is tractable, then Problem (6)-(8) can be solved efficiently.

This paper proposes an analytical, differentiable and transient network model h (System of Equations (8)), that indeed is computationally efficient to evaluate. The proposed transient network model combines ideas from transient queueing theory, queueing network theory and traffic flow theory. It is analytical and differentiable. The model is formulated as a system of nonlinear equations. The model complexity is linear in the number of links in the network and is independent of the individual link space capacities. Hence, it is a scalable model.

The proposed time-dependent network model extends the time-independent network model of Osorio and Chong (2015), which is described in Section 2.2. Traffic dynamics are described by combining transient queueing theoretic ideas inspired from the works of Morse (1958), Cohen (1982) and Odoni and Roth (1983). These ideas are described in Section 2.3.2. Recently, link models that are both based on transient queueing theory and are fully consistent with traditional deterministic traffic flow theoretic link models have been proposed (e.g., Osorio et al. 2011, Osorio and Flötteröd 2014). Their extension to full network models is a topic of ongoing research.

2.2. Stationary network model

The proposed transient model builds upon the stationary model formulated in Osorio and Chong (2015). The latter model combines ideas from finite capacity queueing network

theory, traffic flow theory and various national transportation norms. The detailed formulation is given in Osorio and Chong (2015). In what follows, we outline the key ideas of the formulation.

Each lane of an urban road network is modeled as one or two queues. In order to account for the limited physical space that a queue of vehicles may occupy, we use *finite capacity queueing theory*, where there is a finite upper bound on the length of each queue. Each queue is an M/M/1/k queue. The queue-length upper bound k is determined by the length of the underlying lane. The network model analytically describes the occurrence and impact of vehicular spillbacks with the queueing-theoretic notion of *blocking*. A vehicular spillback occurs when a lane is full and, hence, blocks or inhibits vehicular arrivals from upstream lanes. The model describes the occurrence of *blocking*, as well as its network-wide impact.

The stationary model is defined as the following system of nonlinear equations, where index i refers to a given queue.

γ_i	external arrival rate;
$\hat{\lambda}_i$	effective arrival rate;
μ_i	service rate;
$\hat{\rho}_i$	effective traffic intensity;
k_i	upper bound of the queue length;
N_i	total number of vehicles in queue i;
$P(N_i = k_i)$	probability of queue i being full, also known as the blocking or spillback probability;
p_{ij}	turning probability from queue i to queue j;
$\mathscr{D}_i$	set of downstream queues of queue i.

$$\begin{cases} \hat{\lambda}_i = \gamma_i(1 - P(N_i = k_i)) + \sum_j p_{ji}\hat{\lambda}_j & \text{(9a)} \\ \hat{\rho}_i = \dfrac{\hat{\lambda}_i}{\mu_i} + \left(\sum_{j\in\mathscr{D}_i} p_{ij}P(N_j = k_j)\right)\left(\sum_{j\in\mathscr{D}_i}\hat{\rho}_j\right) & \text{(9b)} \\ P(N_i = k_i) = \dfrac{1-\hat{\rho}_i}{1-\hat{\rho}_i^{k_i+1}}\hat{\rho}_i^{k_i}. & \text{(9c)} \end{cases}$$

Equation (9a) is a flow conservation equation. It describes flow transmission between upstream and downstream queues. Equation (9b) defines the effective traffic intensity of queue i (denoted $\hat{\rho}_i$). The first term on the right-hand side of Equation (9b) represents the traffic intensity of queue i when none of the queues downstream of queue i spillback. It is given by the ratio of the effective arrival rate of queue i, $\hat{\lambda}_i$, and the service rate of queue i, μ_i. The latter represents the flow capacity of the underlying lane when there are no downstream spillbacks. It is determined from national transportation norms. For instance, for signalized lanes, the service rate is defined as a function of the duration of green time allocated to the underlying lane. The second term on the right-hand side

of Equation (9b) accounts for the occurrence and impact of downstream spillbacks. The effective traffic intensity of queue i, $\hat{\rho}_i$, can be interpreted as the ratio of the expected demand to the expected supply. Equation (9c) defines the probability that queue i is full. This is also referred to as the spillback probability or the blocking probability. This expression is derived from finite capacity queueing theory (e.g., Bocharov et al. 2004).

For a given queue i, the exogenous parameters are γ_i, μ_i, p_{ij} and k_i, the endogenous variables are $\hat{\lambda}_i$, $\hat{\rho}_i$ and $P(N_i = k_i)$. In the signal control problem studied in Section 3.1, the flow capacities, μ_i, of the signalized lanes become endogenous variables. Hereafter, we assume μ_i to be endogenous.

For a network with n queues, this model consists of $3n$ equations. The model complexity is linear in the number of queues, and is independent of the space capacity of the queues. This has made it suitable for the analysis of large-scale problems.

2.3. Transient network model

The stationary model uses time-independent endogenous variables and parameters. It does not provide any temporal information, and is therefore not suitable to address dynamic optimization problems. In this paper, we propose a transient network model. This model is then used to approximate the physical component of the metamodel, i.e., f_A of Equation (5). The transient metamodel is used in Section 4 to address a dynamic SO problem.

This section formulates the transient network model. We discretize the time horizon of interest into a set $\mathcal{L}$ of disjoint equal-length time intervals. In this section, we present the model formulation for a given time interval ℓ, $\ell \in \mathcal{L}$.

Section 2.3.1 defines, for interval ℓ, a set of endogenous queueing variables. Section 2.3.2 and 2.3.3 describe how these variables are used to derive time-dependent spillback probabilities, which describe traffic dynamics throughout the network.

2.3.1. Interval-specific queueing variables

The proposed transient model extends the above stationary model by accounting for the temporal variations of the spillback probability. For a given time interval ℓ and queue i, we consider the following interval-specific variables:

$\hat{\lambda}_{i,\ell}$	effective arrival rate;
$\hat{\rho}_{i,\ell}$	effective traffic intensity;
$\mu_{i,\ell}$	service rate;
$P_\ell(N_i = k_i)$	stationary spillback probability.

These variables are defined by solving the following system of equations:

$$\begin{cases} \hat{\lambda}_{i,\ell} = \gamma_i(1 - P_\ell(N_i = k_i)) + \sum_j p_{ji}\hat{\lambda}_{j,\ell} & \text{(10a)} \\ \hat{\rho}_{i,\ell} = \dfrac{\hat{\lambda}_{i,\ell}}{\mu_{i,\ell}} + \left(\sum_{j\in\mathscr{D}_i} p_{ij} P_\ell(N_j = k_j)\right)\left(\sum_{j\in\mathscr{D}_i} \hat{\rho}_{j,\ell}\right) & \text{(10b)} \\ P_\ell(N_i = k_i) = \dfrac{1-\hat{\rho}_{i,\ell}}{1-\hat{\rho}_{i,\ell}^{k_i+1}}\hat{\rho}_{i,\ell}^{k_i}. & \text{(10c)} \end{cases}$$

This system of equations is the interval-specific version of the System of Equations (9). It assumes that the exogenous parameters (γ_i, p_{ij} and k_i) do not change across time intervals. This assumption can be easily relaxed. By solving the above system of equations, we obtain interval-specific endogenous variables for each queue: $\hat{\lambda}_{i,\ell}$, $\hat{\rho}_{i,\ell}$ and $P_\ell(N_i = k_i)$. These variables may vary from one time interval to the next, yet are assumed constant within a time interval. This assumption significantly reduces model complexity and preserves model tractability.

In the case study of this paper, the decision vector consists of the green times of the signalized lanes. There is a one-to-one mapping between the total green time of a lane and the service rate of the corresponding queue (denoted $\mu_{i,\ell}$). Given a specific decision vector value (and hence a specific set of $\mu_{i,\ell}$ values), the above System of Equations (10) can be solved simultaneously for all queues, yet independently for each time interval. Therefore, given a decision vector value, a set of L decoupled systems of equations can be solved to obtain the endogenous variables for all time intervals. The formulation of these variables as decoupled systems of equations contributes to the tractability and scalability of the proposed formulation.

Consider a network with a total of n queues. For a given decision vector value and a given time-interval ℓ, the System of Equations (10) consists of a total of $3n$ variables, $3n$ equations: n linear (10a), n quadratic (10b) and n non-quadratic convex (10c). The system can therefore be solved efficiently. For any feasible set of demand and supply parameters, i.e., $\{\gamma \geq 0, \mu \geq 0\}$, the system contains at least one solution. In particular, the use of finite capacity queues ensures that for any positive value of the traffic intensity (i.e., the ratio of the expected demand to the expected supply) of each queue, there exists a stationary regime for the network of queues, and hence the stationary probabilities are well-defined. If we had resorted to the use of infinite capacity queues, then the traffic intensities would need to be strictly smaller than 1 to ensure stationarity.

2.3.2. Observations from existing transient queueing models

The goal is to describe the temporal variations of the spillback probabilities. Such time-dependent probabilities are referred to in queueing theory as transient probabilities. In the

field of transportation, models based on transient queueing theory have focused on infinite capacity queues: Heidemann (2001), Peterson et al. (1995) and Odoni and Roth (1983). More broadly, in the field of queueing network theory, research has focused mostly on: (i) networks with infinite capacity queues, and (ii) the analysis of the stationary regime. This is, arguably, because between-queue (i.e., spatial) dependencies are intricate to describe analytically, let alone their temporal variations.

The analytical transient analysis of a single isolated finite capacity queue is presented in the seminal work of Morse (1958) and Cohen (1982). The formulation of the proposed transient network model builds upon ideas from these two works.

Morse (1958) considers an isolated M/M/1/k queue, with fixed arrival rate λ, service rate μ, traffic intensity $\rho = \lambda/\mu$, and a given queue-length distribution at the beginning of a time interval (i.e., initial conditions). The latter is called the initial queue-length distribution. We denote the beginning of the time interval by t_0. Morse (1958, Equation (6.13)) derives an exact closed-form expression for the transient queue-length distribution. More specifically, t time units after t_0, the probability of observing a queue of length m is given by:

$$\begin{cases} P(N=m,t) = P(N=m) + \dots \\ \quad \dots + \rho^{\frac{m}{2}} \displaystyle\sum_{s=1}^{k} C_s \left[\sin\left(\frac{sm\pi}{k+1}\right) - \sqrt{\rho}\sin\left(\frac{s(m+1)\pi}{k+1}\right) \right] e^{-w_s t} & \text{(11a)} \\ w_s = \lambda + \mu - 2\sqrt{\lambda\mu}\cos\left(\frac{s\pi}{k+1}\right). & \text{(11b)} \end{cases}$$

The probability that the queue is of length m at time t is denoted $P(N=m,t)$, which is also known as the transient probability. The corresponding stationary probability is denoted $P(N=m)$. The coefficients C_s are determined by solving a linear system of equations that ensure initial boundary conditions:

$$P(N=m,0) = P^0(N=m), \tag{12}$$

where $P^0(N=m)$ denotes the given initial conditions, i.e., the probability that the queue is of length m at time t_0.

The System of Equations (11) could be used within a network setting in order to approximate the marginal queue-length distribution of each queue in a network. The main challenge of such an approach is that in order to compute the coefficients C_s, the full queue-length distribution of each queue would need to be computed. In other words, for each queue i, a set of $k_i + 1$ probabilities would need to be computed, and this for every time interval. This would lead to a model complexity that depends on the space capacity, k_i, of each queue. For instance, in a network with n queues, and a problem with L time

intervals, the total number of probabilities to approximate would be $\sum_{i=1}^{n}(k_i+1)L$. Such an approach would not scale well for large-scale urban networks.

The factor $1/w_s$ of Equation (11a) is known in queueing theory as the *relaxation time*. It is the time needed for a given performance metric to reach its stationary value. Equation (11a) states that the transient queue length distribution converges exponentially to the stationary distribution. Seminal papers that have studied the relaxation time of an isolated infinite capacity queue include Cohen (1982) and Odoni and Roth (1983), where the exponential decay term is written as $e^{-t/\tilde{\tau}}$, and $\tilde{\tau}$ is the relaxation time. Cohen (1982) considers an isolated M/M/1 queue and proposes:

$$\tilde{\tau} = 1/(\mu(1-\sqrt{\rho})^2). \tag{13}$$

Odoni and Roth (1983) propose an approximation of $\tilde{\tau}$ for an isolated G/G/1 queue. For an M/M/1 queue, their approximation is similar to that of Cohen (1982) and is given by: $\tilde{\tau} = 2/(2.8\mu(1-\sqrt{\rho})^2)$.

These approximations share the following properties, which will be preserved in our proposed relaxation time approximation.

- The relaxation time increases as congestion increases (for an infinite capacity queue the stationary state is only defined if $\rho < 1$, and increasing congestion corresponds to $\rho \to 1$).
- For a fixed traffic intensity ρ, the relaxation time should be proportional to the time units of the queueing system parameters. In other words, it should be inversely proportion to either the arrival or the service rates. For example, in the above approximations, $\tilde{\tau}$ is proportional to $1/\mu$.

2.3.3. Transient queueing model

This section formulates a transient queueing model that preserves the following properties of the stationary queueing model of Section 2.2.

- The focus is on the approximation of the transient spillback probabilities. In other words, for each time interval ℓ and each queue i, our objective is to approximate $P_\ell(N_i = k_i, t)$ rather than the full distribution. This leads to a model complexity in the order of nL (instead of $\sum_{i=1}^{n}(k_i+1)L$). The model complexity is linear in the number of queues, and more importantly, is independent of the space capacities.
- The between-queue dependencies are captured through the queueing variables $(\hat{\lambda}, \hat{\rho})$. Given these queueing variables, the spillback probability of a given queue does not depend on any information from other queues. These variables describe, respectively, the expected demand and the ratio of expected demand to expected supply. They capture problem structure, and are therefore referred to as structural variables.

- The structural variables of the queues can be derived by solving a simple system of equations.

Consider time interval ℓ that begins at time t_ℓ and a given queue i. The spillback probability t time units after t_ℓ is approximated by:

$$\begin{cases} P_\ell(N_i = k_i, t) = P_\ell(N_i = k_i) + (P_\ell(N_i = k_i, t_\ell) - P_\ell(N_i = k_i))e^{-\frac{t}{\tau_{i,\ell}}} & \text{(14a)} \\ \tau_{i,\ell} = \dfrac{c\hat{\rho}_{i,\ell}k_i}{\hat{\lambda}_{i,\ell}(1-\sqrt{\hat{\rho}_{i,\ell}})^2}. & \text{(14b)} \end{cases}$$

Equation (14a) is inspired from Equation (11a) in that the transient probability of a queue is defined as the sum of its stationary probability (term $P_\ell(N_i = k_i)$) and a term that decays exponentially with time. The stationary probability is defined by the System of Equations (10).

Equation (14b) is inspired from Equation (13) in that the relaxation time is: (i) directly proportional to $1/(1-\sqrt{\hat{\rho}})^2$, and (ii) proportional to the service rate term given by $\hat{\rho}/\hat{\lambda}$. Equation (14b) is inspired from (11b) in that the relaxation time depends on the space capacity k. Note that the works of Cohen (1982) and of Odoni and Roth (1983) consider infinite capacity queues, hence their relaxation time approximations do not depend on space capacity. In Equation (14b), the term c is an exogenous scaling parameter, that is fitted based on traffic simulation outputs.

For any set of feasible initial conditions, (i.e., $0 \leq P_\ell(N_i = k_i, t_\ell) \leq 1$) System (14) converges asymptotically to $P_\ell(N_i = k_i)$. Convergence is guaranteed for any positive value of the traffic intensity (even for values larger than 1).

2.4. Methodology summary

Let us summarize the proposed methodology. A dynamic extension of the metamodel SO framework of Osorio and Bierlaire (2013) is used. The metamodel is defined by Equation (5). The key to developing a computationally efficient SO algorithm lies in the formulation of an analytical and tractable problem-specific approximation (denoted f_A in Equation (5)) of the objective function (denoted f in Equation (1)). This paper proposes a transient queueing network model that yields a tractable approximation of f_A. The model considers, for each time interval ℓ, a set of endogenous queueing model variables defined by the System of Equations (10). These variables approximate the between-queue dependencies, e.g., how spillback at a given queue impacts the performance of upstream queues. Given this set of variables, the spillback probability of each queue varies across time, within time interval ℓ, following Equation (14). The transient queueing network model is then used to derive the functional form of f_A. An example of the derivation of an expression for f_A is given in Section 3.2 for a traffic signal control problem.

Algorithm 1 Algorithm to evaluate the transient network model

Carry out each of the following steps for all queues i before proceeding to the next step.

Steps:

1. define the exogenous parameters $\gamma_i, k_i, p_{ij}, \mu_i$.
2. define the start of each time interval $t_1, t_2, \ldots, t_L$.
3. define the initial condition of each queue: $P(N_i = k_i, t_1)$.
4. repeat the following for time intervals $\ell = 1, 2, \ldots, L$
   (a) solve the System of Equations (10) to obtain $\hat{\lambda}_{i,\ell}, \hat{\rho}_{i,\ell}$ and $P_\ell(N_i = k_i)$.
   (b) compute the spillback probabilities at the end of the time interval according to (14) with $t = t_{\ell+1}$.

An algorithmic summary of the transient network model is given in Algorithm 1. For a network with L time intervals and n queues, the number of endogenous variables is $3nL$. In other words, for each queue and each time interval, the endogenous variables are: $\hat{\lambda}_{i,\ell}$, $\hat{\rho}_{i,\ell}$, and $P_\ell(N_i = k_i)$.

We now summarize the main differences between the proposed transient and the stationary analytical network model of Osorio and Chong (2015). The stationary model yields stationary (hence, time-independent) lane spillback probabilities, while time-dependent probabilities are derived by the transient queueing model. Thus, the proposed model provides a temporal description of congestion propagation. The queueing variables that describe demand and supply (e.g., arrival rates, traffic intensities) are time-independent for the stationary model, they are constant for the entire time horizon. The transient model uses a set of variables for each time period, this allows to describe temporal changes in demand and supply.

The proposed analytical model builds upon the stationary model of Osorio and Chong (2015). For a network with n lanes and a set of L time intervals, the stationary model consists of a system of $3n$ equations with $3n$ endogenous variables, while the transient model consists of a system of L systems of equations that are solved sequentially and each have a dimension $3n$. The transient model consists of $3nL$ endogenous variables. The complexity of the proposed model scales linearly with the number of time intervals. Thus, it is less tractable than the stationary model. The complexity of both models is linear in n and is independent of the link space capacities. This makes them both suitable for large-scale network analysis.

3. Time-dependent traffic signal control problem

The proposed method is suitable to address a variety of simulation-based dynamic transportation problems. In this section, we illustrate the computational efficiency of

the methodology by considering a large-scale traffic signal control problem with time-dependent decision variables. Section 3.1 formulates the traffic control problem. Section 3.2 presents the analytical expression for f_A (of Equation (5)) for this specific problem. Section 3.3 discusses implementation details.

3.1. Optimization problem formulation

A detailed review of traffic signal control terminology is given in Appendix A of Osorio (2010) or in Lin (2011). We consider fixed-time (also called time of day or pre-timed) signal control plans. A fixed-time signal plan is a periodic plan that repeats itself in a certain interval (e.g., evening peak hour). Fixed-time signal plans are pre-determined based on historical or simulation-based traffic patterns. They are determined offline. Unlike traffic-responsive strategies, they do not respond to prevailing real-time traffic conditions. Congested networks with complex traffic dynamics (e.g., grid topology, congested multi-modal traffic) often resort to the use of fixed-time plans (Chen et al. 2015).

We divide the time horizon of interest (e.g., evening peak period) into L time intervals. For each time interval, we determine a fixed-time signal plan. The signal plans for all intersections and all L time intervals are determined jointly.

The main decision variables of fixed-time signal control problems are green splits, cycle lengths and offsets. The cycle length of a given intersection is the period of the signal plan, i.e., the time required to complete one sequence of signals. The green split of a given lane corresponds to the ratio of the total green time allocated to that lane during the cycle and the cycle length. The offsets are defined as the differences in the starting time of a cycle for a sequence of intersections. They enable the coordination of adjacent signals.

This paper focuses on the optimization of green splits, i.e., the decision variables are the green splits of the signal controlled lanes. Cycle lengths and offsets are fixed. All other signal plan variables (e.g., stage structure) are also assumed fixed.

To formulate this problem we introduce the following notation:

b_i	ratio of available cycle time to total cycle time for intersection i;
x_ℓ	vector of green splits for time interval ℓ;
$x_\ell(j)$	green split of signal phase j for time interval ℓ;
x_{LB}	vector of lower bounds for green splits;
$\mathscr{I}$	set of intersection indices;
$\mathscr{P}_I(i)$	set of endogenous signal phase indices of intersection i.

The problem is formulated as follows:

$$\min_{x_1,\ldots,x_L} f(x,y;p) = \frac{1}{L}\sum_{\ell=1}^{L} E[F_\ell(x_\ell, y_\ell; p)] \tag{15}$$

subject to

$$\sum_{j \in \mathscr{P}_I(i)} x_\ell(j) = b_i, \ \forall i \in \mathscr{I}, \ell \in \mathcal{L} \tag{16}$$

$$x_\ell \geq x_{LB}, \ \forall \ell \in \mathcal{L}. \tag{17}$$

The decision vector x consists of the green splits of all signal phases in all L time intervals. The objective is to minimize the expected trip travel time, where $E[F_\ell(x_\ell, z_\ell; p)]$ represents the expected trip travel time during time interval ℓ.

The linear constraints (16) ensure that, for each intersection, the sum of the green times for each signal phase is equal to the available (i.e., non-fixed) cycle time. Equation (17) ensures lower bounds for the green splits. These bounds may vary according to the city, the time horizon of interest, and even the intersection.

3.2. Derivation of the analytical objective function, f_A

Recall that the transient network model of Section 2 is used to derive the analytical approximation (f_A of Equation (5)) of the simulation-based objective function (f of Equation (15)). We now derive the analytical expression for f_A for the specific objective function (15). More specifically, we derive the analytical approximation of the term $E[F_\ell(x_\ell, z_\ell; p)]$ in Equation (15). Let $f_{A,\ell}$ denote this approximation.

For time interval ℓ, we can derive the expected time in the network per user by applying Little's law (Little 1961) to the entire road network. This leads to:

$$f_{A,\ell} = \frac{\sum_i E_\ell[N_i]}{\frac{1}{t_{\ell+1}-t_\ell}\int_{t_\ell}^{t_{\ell+1}} \sum_i \gamma_i (1 - P_\ell(N_i = k_i, t))dt}, \tag{18}$$

where $E_\ell[N_i]$ represents the expected number of vehicles in queue i during time interval ℓ, t_ℓ denotes the start time of time interval ℓ, and $t_{\ell+1}$ denotes the end time of time interval ℓ. The numerator is the expected number of vehicles in the network during time interval ℓ. The denominator is the effective external arrival rate to the network during time interval ℓ. In the denominator, the term within the integral represents the instantaneous effective external arrival rate to queue i at time t. The external arrival rate γ_i is an exogenous parameter, and the transient spillback probability $P_\ell(N_i = k_i, t)$ is given by Equation (14a).

We now derive the closed-form expression used to approximate the numerator of Equation (18), we then derive a closed-form expression for the denominator. The closed-form expression for $E_\ell[N_i]$ of the numerator is derived as follows. For an isolated queue i of the type M/M/1/k_i, with traffic intensity ρ_i, the stationary expected number of vehicles is given by:

$$E[N_i] = \rho_i \left(\frac{1}{1-\rho_i} - \frac{(k_i+1)\rho_i{}^{k_i}}{1-\rho_i{}^{k_i+1}}\right). \tag{19}$$

An analytical derivation of Equation (19) is given in Osorio and Chong (2015). We assume this functional form holds within a given time interval, i.e., we use the following approximation:

$$E_\ell[N_i] = \rho_{i,\ell}\left(\frac{1}{1-\rho_{i,\ell}} - \frac{(k_i+1)\rho_{i,\ell}{}^{k_i}}{1-\rho_{i,\ell}{}^{k_i+1}}\right). \tag{20}$$

An analytical expression for $\rho_{i,\ell}$ is obtained as follows. The model of Osorio and Chong (2015) (presented in Section 2.2 of this paper) is formulated based on the effective traffic intensity $\hat{\rho}_i$, rather than the traffic intensity ρ_i of a queue. The effective traffic intensity is related to the traffic intensity ρ_i as follows: $\rho_i = \hat{\rho}_i/(1 - P(N_i = k_i))$. We therefore approximate the traffic intensity of queue i during time-interval ℓ by:

$$\rho_{i,\ell} = \frac{\hat{\rho}_{i,\ell}}{\frac{1}{t_{\ell+1}-t_\ell}\int_{t_\ell}^{t_{\ell+1}}(1 - P_\ell(N_i = k_i, t))dt}, \tag{21}$$

where $\hat{\rho}_{i,\ell}$ is defined by Equation (10b). A closed-form expression for the integral in the denominator of Equation (21) is obtained as follows. We insert the expression for $P_\ell(N_i = k_i, t)$ given by Equation (14a) to obtain:

$$A = \int_{t_\ell}^{t_{\ell+1}} (1 - P_\ell(N_i = k_i, t))\, dt \tag{22}$$

$$= \int_{t_\ell}^{t_{\ell+1}} \left(1 - \left[P_\ell(N_i = k_i) + (P_\ell(N_i = k_i, t_\ell) - P_\ell(N_i = k_i))\, e^{-\frac{t}{\tau_{i,\ell}}}\right]\right) dt \tag{23}$$

$$= \int_{t_\ell}^{t_{\ell+1}} (1 - P_\ell(N_i = k_i))\, dt - (P_\ell(N_i = k_i, t_\ell) - P_\ell(N_i = k_i)) \int_{t_\ell}^{t_{\ell+1}} e^{-\frac{t}{\tau_{i,\ell}}} dt \tag{24}$$

$$= (t_{\ell+1} - t_\ell)(1 - P_\ell(N_i = k_i)) + \tau_{i,\ell}(P_\ell(N_i = k_i, t_\ell) - P_\ell(N_i = k_i))(e^{-\frac{t_{\ell+1}}{\tau_{i,\ell}}} - e^{-\frac{t_\ell}{\tau_{i,\ell}}}) \tag{25}$$

In summary, the term $E_\ell[N_i]$ of the numerator of Equation (18) is given by Equations (20), (21) and (25).

The denominator of Equation (18) can be rewritten by interchanging the summation with the integral to obtain:

$$B = \frac{1}{t_{\ell+1}-t_\ell}\int_{t_\ell}^{t_{\ell+1}} \sum_i \gamma_i (1 - P_\ell(N_i = k_i, t))dt \tag{26}$$

$$= \frac{1}{t_{\ell+1}-t_\ell}\sum_i \gamma_i \int_{t_\ell}^{t_{\ell+1}} (1 - P_\ell(N_i = k_i, t))dt. \tag{27}$$

A closed-form expression for the integral of Equation (27) is given by Equation (25).

Note that the analytical expressions derived above allow us to approximate the expected trip travel time (i.e., the objective function) based on the knowledge of spillback probabilities $P_\ell(N_i = k_i, t)$ rather than the knowledge of full queue-length distributions. This contributes to the tractability and scalability of the proposed approach. This leads to a model complexity that is linear in the number of queues and that is independent of the space capacity of each queue.

3.3. Implementation notes

We implement the lower bound constraints (17) as nonlinear equality constraints by introducing a new variable v and implementing:

$$x_\ell = x_{LB} + v_\ell^2. \tag{28}$$

In addition, we enforce the positivity of the endogenous variables $\hat{\rho}_{i,\ell}$ by introducing a new variable $u_{i,\ell}$ and adding the equalities:

$$\hat{\rho}_{i,\ell} = u_{i,\ell}^2. \tag{29}$$

We do not enforce the positivity of the other endogenous variables, rather we check a posteriori that all other endogenous variables are positive. In our numerous experiments, all solutions to the system of equations obtained by the solver have consisted of positive values.

Note that the green splits are related to the service rate of the underlying queue i through the following equation:

$$\mu_{i,\ell} = \left(e_i + \sum_{j \in \mathscr{P}_I(i)} x_\ell(j) \right) s, \tag{30}$$

where $\mathscr{P}_I(i)$ represents the set of endogenous phase indices of the lane represented by queue i, e_i is the ratio of fixed green time to cycle time of signalized queue i, and s is the saturation flow rate. We assume a common saturation flow for all signalized lanes. For each signalized queue, Equation (30) is inserted into Equation (10b), in order to implement both constraints as a single constraint.

In order to further enhance tractability, for the large-scale case study of Section 4, we approximate the arrival rate to each queue (denoted $\hat{\lambda}_{i,\ell}$) as exogenous; i.e., it does not vary with the decision vector values. The exogenous value is obtained by considering the prevailing fixed-time signal plan of the city for the whole time horizon, this yields a set of $\mu_{i,\ell}$ values (through Equation (30)). Then the System of Equations (10) is solved, and the corresponding $\hat{\lambda}_{i,\ell}$ values obtained are used as fixed values throughout the optimization. This simplification enhances model tractability. Nonetheless, the assumption of arrival patterns to the links independent of the signal plans may lead to a misestimation of the link spillback probabilities. Appendix C derives, as an example, the expression of the derivative of the objective function with regards to an endogenous variable.

For a problem with L time intervals, n lanes (where each lane is modeled as a single queue), where we determine r endogenous signal phases at a total of o signalized intersections per time interval, our implementation leads to a total of $(2n + r)L$ endogenous

variables. These consist of two endogenous queueing variables per queue per time interval ($u_{i,\ell}$ and $P_\ell(N_i = k_i)$), and one green split variable ($v_l(j)$) for each signal phase. The corresponding optimization problem (i.e., a trust region subproblem) solved at every iteration of the SO algorithm consists of $(2n + o)L$ nonlinear equality constraints and one nonlinear inequality constraint (which is the trust region constraint). Of the nonlinear equality constraints, $2nL$ correspond to Equations (10b) and (10c), and oL correspond to Equation (16) (the latter becomes nonlinear since v_ℓ is implemented instead of x_ℓ). The trust region (TR) subproblem, that is solved at every iteration, is a variation of the signal control problem formulated in Section 3.1. The detailed formulation of the TR subproblem is described in Appendix B.

4. Lausanne city case study

This section addresses a traffic signal control problem for the city of Lausanne, Switzerland. Section 4.1 describes the network. Section 4.2 benchmarks the proposed transient metamodel SO method against the stationary metamodel SO method proposed by Osorio and Chong (2015). Sections 4.3 and 4.4, respectively, compare the performance of a signal plan derived by the proposed method to that of an existing signal plan for the city of Lausanne, and to that of a signal plan derived by a mainstream commercial signal control software.

4.1. Network

We evaluate the performance of the proposed SO algorithm by considering a large-scale signal control problem for the entire Swiss city of Lausanne. The city map is displayed in Figure 2(a), the considered area is delimited in white. We use a microscopic traffic simulation model of the Lausanne city developed by Dumont and Bert (2006). It is implemented with the Aimsun simulator (TSS 2011), and is calibrated for evening peak period demand. The modeled road network is displayed in Figure 2(b).

Details regarding this Lausanne network are given in Osorio (2010, Chap. 4). We consider the first hour of the evening peak period: 5-6 pm. During this hour, congestion gradually builds up. Hence, it is important to design a signal plan that accounts for this temporal propagation of congestion. We use the proposed algorithm to determine one signal plan for 5-5:30 pm and a second signal plan for 5:30-6 pm. In other words, we decompose the hour into two 30-minute intervals, and determine a signal plan for each of the two intervals.

The road network consists of 603 links and 231 intersections. The signals of 17 intersections are controlled in this case study. These 17 intersections are depicted as filled squares in Figure 2(b). The controlled intersections are located throughout the entire city. The

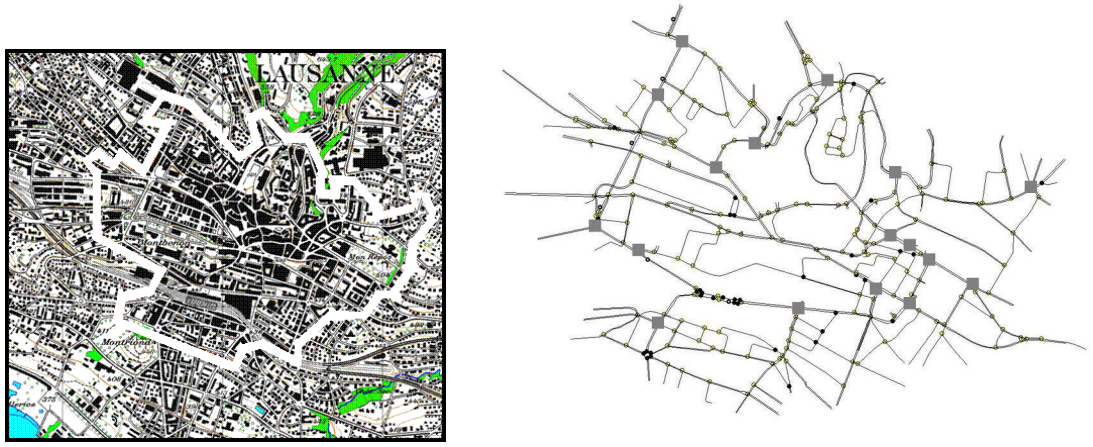

(a) Lausanne city road network (adapted from Dumont and Bert (2006))

(b) Lausanne network model

Figure 2 Lausanne city network and network model

cycle times of these intersections are 80 seconds (for 2 intersections), 90 seconds (for 13 intersections) and 100 seconds (for 2 intersections). The signal control problem has a total of 198 endogenous signal phase variables (99 signal phases per time interval), i.e., the dimension of the decision vector is 198. The phase variable is defined as the ratio of green time (i.e., the total duration of a phase) to cycle time.

The transient queueing model of this network consists of 902 queues. The trust region (TR) subproblem solved at every iteration of the SO algorithm consists of 3806 endogenous variables with 3642 nonlinear equality constraints, and one trust region inequality. The lower bounds of the green splits (Equation (17)) are set to 4 seconds according to the Swiss transportation norm (VSS 1992).

In the field of urban traffic signal control, networks in the order of 70 links and 16 controlled intersections are considered large-scale problems (Aboudolas et al. 2010, 2007, Dinopoulou et al. 2006). The problem considered in this paper is therefore a large-scale signal control problem. The SO algorithm of this paper is based on the use of a derivative-free algorithm. Unconstrained deterministic problems in the order of 200 variables are considered large-scale for derivative-free algorithms (Conn et al. 2009). Additionally, the considered problem is constrained and simulation-based, it is particularly difficult to address.

4.2. Comparison of the dynamic SO method with the stationary SO method

In order to benchmark the performance of the dynamic SO (DSO) method, we compare its performance to that of an SO method that has been successfully used to address large-scale SO problems. We benchmark the performance of the dynamic SO method against the performance of the stationary SO (SSO) method proposed in Osorio and

Table 1 Traffic models used by each of the compared SO methods.

	Microscopic simulation-based	Macroscopic analytical stationary	Macroscopic analytical transient
Dynamic SO	✓		✓
Stationary SO	✓	✓	

Chong (2015). Both methods consider a metamodel defined by Equation (5). They differ only in the physical component of the metamodel (f_A of Equation (5)). The proposed DSO method considers the transient network model formulated in Section 2.3. The SSO method considers the stationary network model defined by the System of Equations (9). All other algorithmic details and parameters are identical in both methods. The difference between these two methods is also described in Table 1. This comparison allows us to evaluate and quantify the added value of using transient analytical information in the metamodel (i.e., the added value of using a time-dependent network model to derive f_A of Equation (5)).

For both methods, we consider a tight computational budget, which is defined as a maximum of 100 simulation runs that can be carried out. In other words, the SO algorithm is initialized with no simulation observations available, and it stops once a total of 100 simulation runs have been carried out. We refer the readers to Osorio and Chong (2015) for more information about the SSO algorithm, and for a comparison of its performance to that of a traditional SO algorithm.

We consider four different initial points (i.e., initial signal plans) to initialize the SO algorithms. These points are uniformly randomly drawn from the feasible space defined by Equations (16) and (17). This uniform sampling is carried out according to the code of Stafford (2006). For each initial point, we run each SO method (i.e., SSO and DSO) three times, each time allowing for a total of 100 simulation runs. Thus, for each method and each initial point, we derive three *proposed* signal plans. In order to evaluate the performance of a proposed signal plan, we embed it within the traffic simulator and run 50 simulation replications. We then compare the performance of the proposed signal plans both with statistical tests, and by comparing the cumulative distribution function (cdf) of the objective function realizations (i.e., the average trip travel times) obtained from these 50 simulation replications.

Each plot of Figure 3 considers a different initial point. Each curve of each plot displays the cdf of a given signal plan. For each plot, the x-axis displays the average trip travel time (ATTT). For a given x value, the y-axis displays the proportion of simulation replications (out of the 50 replications) that have ATTT values smaller than x. Hence, the more a cdf curve is located to the left, the higher the proportion of small ATTT values; i.e., the better the performance of the corresponding signal plan.

For each plot, the solid thick curve corresponds to the cdf of the initial signal plan, the solid thin curves are the cdf's of signal plans proposed by DSO and the dashed curves are the cdf's of signal plans proposed by SSO.

For all four initial points (Figures 3(a)-3(d)), all three plans derived by both DSO and SSO yield improved performance when compared to the initial signal plan. For three of the four initial points (Figures 3(a)-3(c)), all three plans derived by DSO outperform all three plans derived by SSO. For Figure 3(d), two out of the three DSO plans outperform all three SSO plans. The third DSO plan performs similarly to two of the SSO plans. It outperforms the third plan proposed by SSO.

In summary, for all four initial points, DSO systematically derives signal plans with improved performance when compared to the initial plan, and most often, when compared to the plans derived by SSO.

We study the robustness of the DSO solutions to the initial points. Figure 4 displays the cdf's of the 12 solutions derived by DSO (solid thin curves) and all 4 initial points (solid thick curves). In other words, all curves of all four plots of Figure 3 are displayed here in a single plot in Figure 4. The plot shows that: (i) the DSO solutions systematically outperform the initial solutions, (ii) all DSO solutions have similar performance. The DSO plans have good and consistent performance across all SO runs and all initial points. This illustrates the robustness of the proposed method to both the initial points and to the stochasticity of the simulator.

In order to test whether the performance of DSO is statistically significantly better than that of SSO, we carry out, for each initial point, a one-sided paired t-test. We choose a performance metric that accounts for the overall performance of an SO method over all three SO runs. The 50 simulation replications used to derive each of the cdf curves of Figure 3 use the same 50 random seeds. Hence, we use a statistic that aggregates the performance of a given SO method for a given random seed. For a given SO method, let X_{ij} denote the average travel time obtained under the j^{th} run ($j \in \{1,2,3\}$) and the i^{th} simulation replication seed ($i \in \{1,2,\ldots,50\}$). The considered performance metric is defined as:

$$Y_i = \frac{1}{3}\sum_{j=1}^{3} X_{ij},\ \forall i \in \{1,2,\ldots,50\}. \tag{31}$$

We treat Y_i as the *average* algorithmic performance of an SO method (DSO or SSO) under replication i.

We use a paired one-sided t-test that assumes that the simulation observations are independent and arise from a normal distribution with common but unknown variance. We pair the observations with common random replication seeds. The null hypothesis

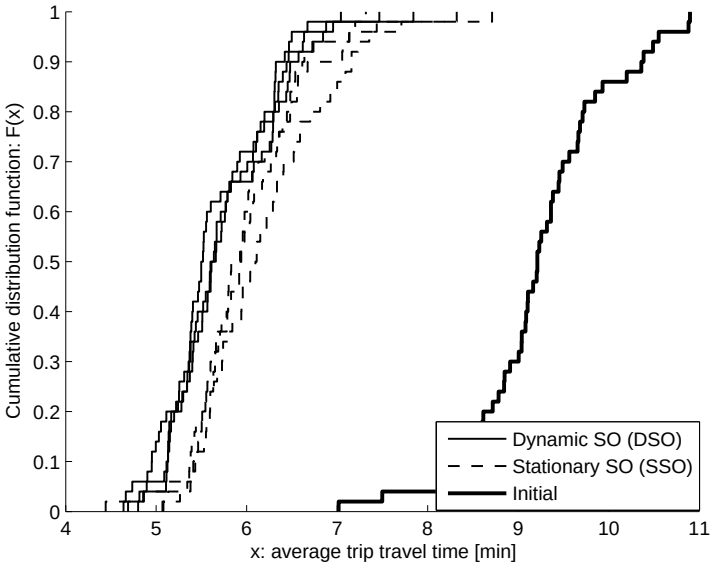

(a) Initial point 1

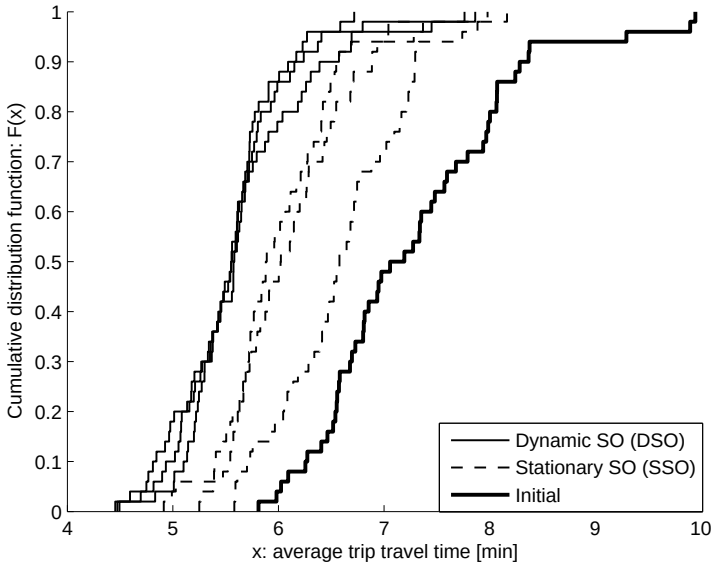

(b) Initial point 2

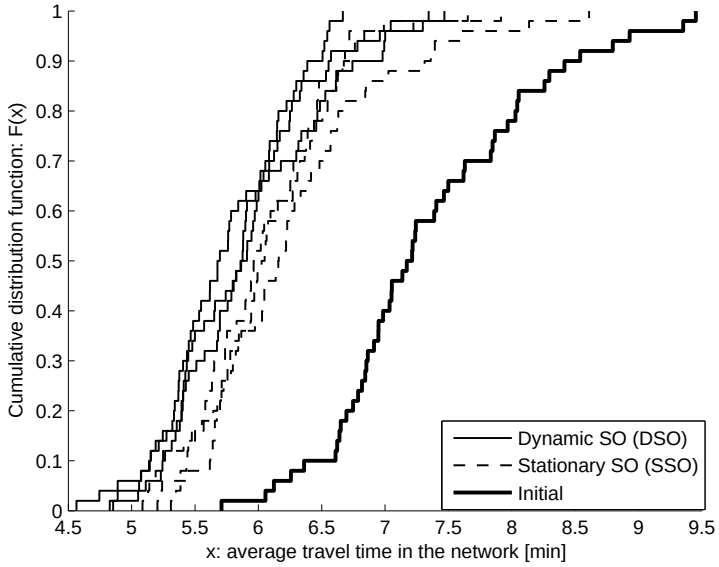

(c) Initial point 3

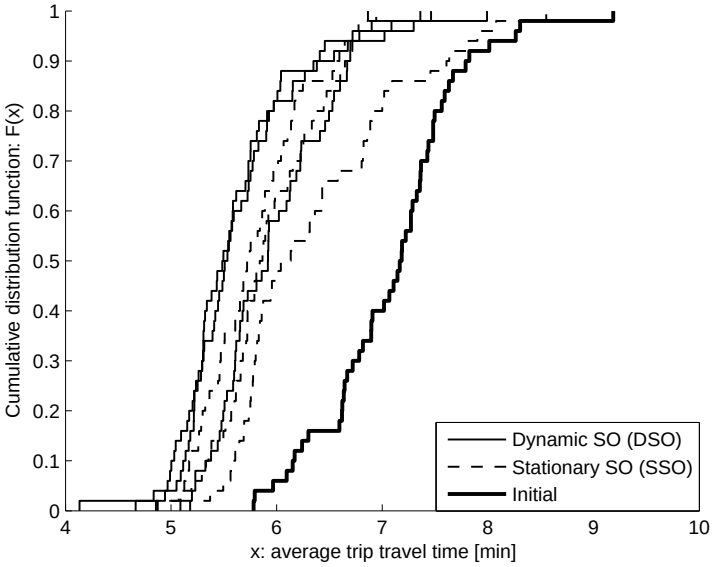

(d) Initial point 4

Figure 3: Cumulative distribution functions of the average travel times considering different initial signal plans.

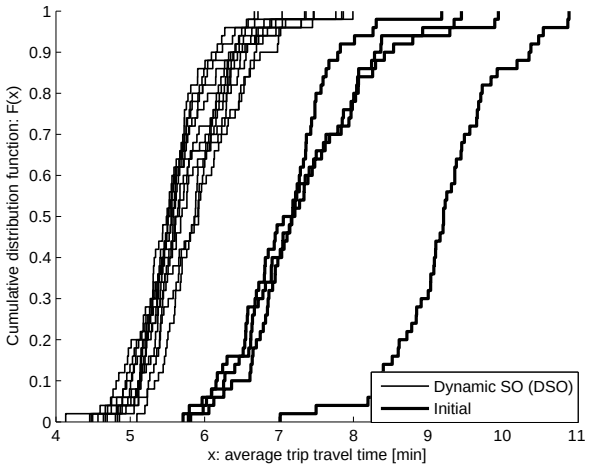

Figure 4 **Cumulative distribution functions of the average travel times for all 4 initial points and all 12 proposed solutions**

Table 2 **Paired one-sided t-test results that compare the performance of DSO and of SSO**

Initial point	T-statistic	P-value	Average	Standard deviation
1	-4.23	$5e-5$	-0.35	0.58
2	-9.31	$1e-12$	-0.65	0.49
3	-3.92	$1e-4$	-0.28	0.51
4	-4.01	$1e-4$	-0.26	0.46

assumes equal expected trip travel times for both DSO and SSO (i.e., equal expected value of Y for each method). The alternative hypothesis assumes that the expectation of the DSO method is lower than that of the SSO method.

The test significance level is 0.05. It has 49 degrees of freedom. The corresponding critical value is -1.677. Table 2 summarizes the test statistics. Each row of the table displays the result of the t-test for a given initial point (i.e., one test for each plot of Figure 3). Columns 1 to 5 display, respectively, the initial point index, the t-statistic, the p-value, the average paired difference and the standard deviation of the paired differences.

All t-statistics (Column 2) are smaller than -1.677, hence the null hypothesis of all four tests is rejected. In other words, for each initial point, the signal plans derived by DSO lead to average travel times that are statistically significantly lower than those of the signal plans derived by SSO.

Performance under increasing congestion levels

We now analyze how the performance of the proposed signal plans varies over time. The traffic simulation considers the first hour of peak period traffic (5-6 pm). Over this hour, congestion gradually increases (for more details regarding the temporal evolution of congestion in this network, see Osorio (2010, Chap. 4)). This temporal analysis allows us to

understand how the proposed signal plans perform under increasingly congested conditions.

For a given signal plan, we estimate the expected trip travel time in ten minute increments. In other words, we consider 6 time windows indexed, respectively, 1 through 6. The corresponding time windows are 5-5:10, 5-5:20, 5-5:30, 5-5:40, 5-5:50 and 5-6 pm.

In Figure 5, each plot displays the results considering the same initial plans and the same *proposed* signal plans as in Figure 3. The x-axis corresponds to the time window index. The y-axis represents the average trip travel time during the corresponding time window. These are averages obtained over the same 50 simulation replications used in the previous analysis. Each of the solid curves corresponds to one of the three signal plans proposed by DSO. Each of the dashed curves corresponds to one of the three signal plans proposed by SSO. In each curve, the dots represent the average travel time during the corresponding time windows. The curves are interpolated from the dots.

Note that the average travel time estimate for the last time window (time window 6) is the trip travel time averaged over all trips from 5-6 pm. This corresponds to an estimate of the objective function of the optimization problem. This estimate also equals the average of all 50 simulation replications points used to construct a given cdf curve of Figure 3.

In Figures 5(a), 5(b) and 5(c), all three plans derived by DSO have better performance compared to the three plans of SSO throughout all six time windows. This holds for two of the three plans derived by DSO in Figure 5(d). In Figure 5(d), the third plan derived by DSO has worse performance than the three SSO plans for the first three time windows, and worse performance than two of the SSO plans for the remaining three time windows. For all DSO plans of Figures 5(a), 5(b) and 5(c), their performance seems stable for congested conditions (time windows 4-6). Overall, the difference in performance between the DSO plans and the SSO plans seems to increase with increasing levels of congestion. This illustrates again the added value of using an analytical model that is time-dependent, such that it describes this temporal evolution of congestion within the time horizon of interest (5-6 pm).

In order to test the statistical significance of the difference in performance over time, we proceed as before: we carry out for each initial point and each time window a paired one-sided t-test. For each t-test, the metric we use is the *average* algorithmic performance of an SO method (DSO or SSO) during the corresponding time window.

Table 3 contains four subtables (a)-(d) that display, respectively, the corresponding t-test statistics, the p-values, the average paired difference and the standard deviation of the paired differences. For a given table, a row corresponds to an initial point, a column

(a) Initial point 1

(b) Initial point 2

(c) Initial point 3

(d) Initial point 4

Figure 5: Time-dependent average trip travel times for different initial signal plans

Table 3 Paired one-sided t-tests that compare the time-dependent performance of DSO and of SSO

(a) T-statistics

Initial point	Time window index 1	2	3	4	5	6
1	-9.64	-8.95	-5.11	-4.36	-4.36	-4.23
2	-16.31	-13.42	-10.84	-9.56	-9.28	-9.31
3	-9.78	-7.97	-5.37	-4.33	-4.11	-3.92
4	0.38	-1.55	-1.83	-2.59	-3.58	-4.01

(b) P-values

Initial point	Time window index 1	2	3	4	5	6
1	$3e-13$	$3e-12$	$3e-6$	$3e-5$	$3e-5$	$5e-5$
2	$9e-22$	$2e-18$	$6e-15$	$4e-13$	$1e-12$	$1e-12$
3	$2e-13$	$1e-10$	$1e-6$	$4e-5$	$7e-5$	$1e-4$
4	0.65	0.063	0.036	0.006	$4e-4$	$1e-4$

(c) Average paired differences

Initial point	Time window index 1	2	3	4	5	6
1	-0.14	-0.25	-0.25	-0.29	-0.34	-0.35
2	-0.24	-0.37	-0.43	-0.50	-0.57	-0.65
3	-0.13	-0.21	-0.21	-0.23	-0.25	-0.28
4	-0.01	-0.04	-0.07	-0.13	-0.21	-0.26

(d) Standard deviation of paired differences

Initial point	Time window index 1	2	3	4	5	6
1	0.1	0.19	0.35	0.47	0.55	0.58
2	0.1	0.2	0.28	0.37	0.43	0.49
3	0.1	0.19	0.28	0.37	0.44	0.51
4	0.11	0.18	0.25	0.35	0.42	0.46

corresponds to a time window. As before, the test significance level is 0.05, it has 49 degrees of freedom, and the critical t-value is -1.677.

Table 3(b) (or equivalently Table 3(a)) shows that for initial point 1, 2 and 3, the null hypothesis of equal expectation for DSO and SSO is rejected for initial points 1, 2 and 3, at all time windows. This means that as congestion increases (i.e., as time advances from 5 pm to 6 pm), the DSO signal plans consistently outperform the SSO plans. For initial point 4, the null hypothesis is rejected for time windows 3-6, and not rejected for time windows 1 and 2. This means that for initial point 4 at low levels of congestion (i.e., the first 20 minutes of the peak hour), the DSO plans do not outperform the SSO plans. Additionally, Table 3(c) shows that for a given initial point (i.e., a given row), the average difference increases with the time window index. This shows that the difference in performance between DSO and SSO increases as congestion increases.

Computational runtime of DSO

The steps of the DSO algorithm that are the most computationally demanding are: (i) evaluating the simulator, and (ii) solving the trust region (TR) subproblem. Details on the formulation and numerical solver used to solve the TR subproblem are given in Appendix B. To illustrate the computational runtimes for each of these steps, we consider the 3 SO runs of the DSO method carried out with initial point 2. Each of the 3 SO runs allows for 100 simulation evaluations. We use a standard laptop with an Inter(R) Core(TM) i7-2960XM 2.7 GHz processor and 8GB RAM. The average runtime for one simulation replication is 1.2 minutes with a standard deviation of 0.2 minutes. The average time to solve the TR subproblem is 5.5 minutes with a standard deviation of 3.6 minutes. These runtimes are suitable for solving the problem offline. As part of ongoing work, we are formulating real-time SO frameworks, where the runtime of both steps needs to be improved. For

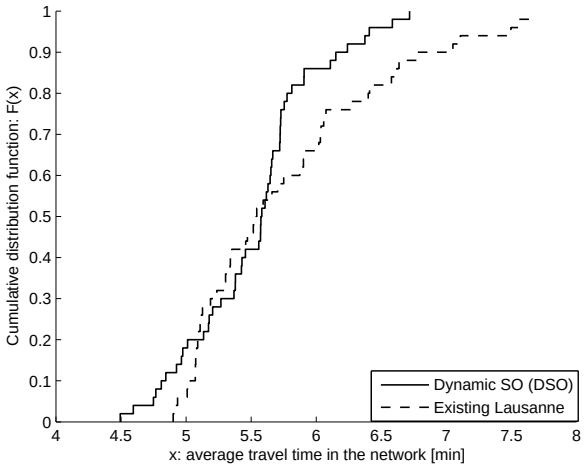

Figure 6 **Comparison of the performance of a DSO signal plan and an existing signal plan of the city of Lausanne**

instance, we currently use the standard Matlab routine for nonlinear constrained problems (*fmincon*) to solve the TR subproblem. The use of a standard TR method would reduce the computational runtime for solving the TR subproblem. For real-time SO methods, the main runtime constraint remains the number of sequential simulation evaluations that can be carried out in real-time.

4.3. Comparison with an existing signal plan of the city of Lausanne

We now compare the performance of the best signal plan derived by DSO with that of an existing signal plan for the city of Lausanne. The best DSO signal plan is defined as the one (among the 12 DSO signal plans analyzed in the previous section) with the lowest average travel time over the 50 simulation replications. This corresponds to the left-most cdf curve of Figure 3(b), or equivalently the signal plan with the smallest y-value at time window 6 of Figure 5(b). Figure 6 displays the cdf of this DSO plan (solid line) and of the Lausanne plan (dashed line). The DSO plan outperforms the Lausanne plan. In order to test whether these differences are statistically significant, we carry out a paired one-sided t-test as before. The t-test has, once again, a significance level of 0.05, 49 degrees of freedom, and a critical value of -1.677. The average trip travel time (average over all 50 simulation replications) of the DSO plan is 5.52 minutes, and that of Lausanne signal plan is 5.77 minutes. The average paired difference is 0.25, the corresponding standard deviation is 0.94. This leads to a t-statistic of -1.83, and a p-value of 0.037. The hull hypothesis is rejected. Therefore, the DSO approach can derive signal plans that perform significantly better than the Lausanne plan.

We now compare the values of the signal plans of the best DSO plan, the best SSO plan and the current Lausanne plan. The best DSO plan is defined as that with the lowest

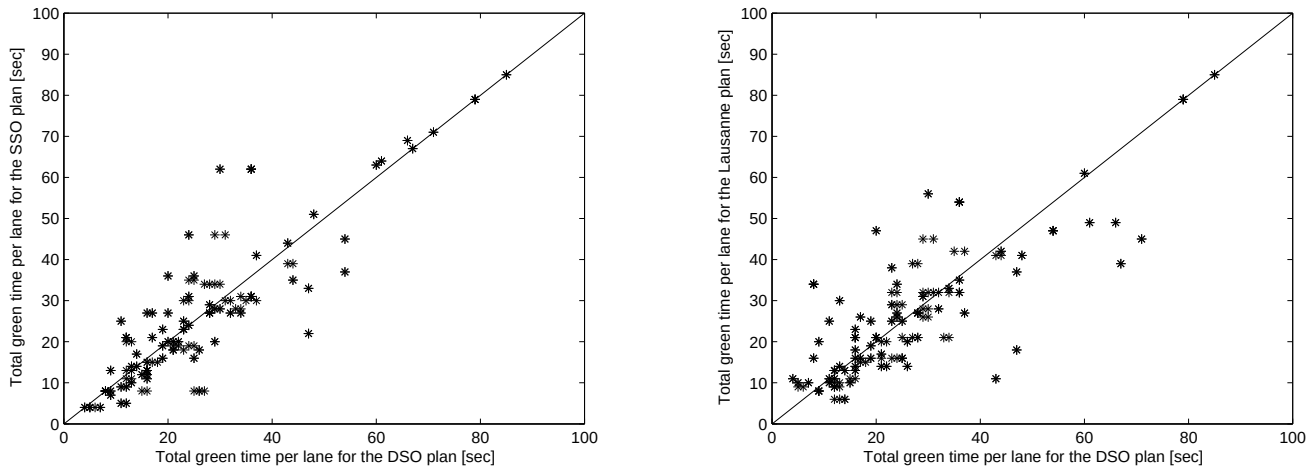

(a) Comparison of the best DSO and the best SSO signal plans (b) Comparison of the best DSO and the Lausanne plans

Figure 7 Total green time (in seconds) per signalized lane for the best DSO, the best SSO and the Lausanne signal plans

average travel time over the 50 simulation replications. This corresponds to the left-most cdf curve of Figure 3(b). Similarly, the best SSO plan is the left-most dashed cdf curve in Figure 3(d).

The x-axis of Figure 7(a) displays, for each signal controlled lane at a time interval, the total green time (in seconds), under the DSO plan. Since the DSO plan yields two different plans for the two intervals, Figure 7(a) displays one point for each of these two time intervals. The y-axis displays the total green time under the SSO plan. The diagonal line $y = x$ is also plotted. The points close to the diagonal line indicate lanes that have similar green time values under both plans. Similarly, Figure 7(b) displays the green times for the DSO plan (x-axis) and the Lausanne plan (y-axis). The plots indicate that there are many lanes with significantly different green times. We have also studied the variations of the green times over time for the DSO plan, but have not found any interesting temporal trends.

Figure 8(a) displays, for each of these 3 signal plans, the average trip travel time as a function of time. Figure 8(b) displays the average link density of the 60 controlled links. For both plots, the x-axis corresponds to a time window index, and for each estimate, the confidence intervals (obtained from the 50 simulation replications) are displayed. The trip travel time metric of Figure 8(a) is defined just as that of Figure (5). Notice that the objective function corresponds to the average travel time estimated at time interval 6 (i.e., it is the average travel time from 5-6pm). Figure 8(b) displays the average link density of the 60 controlled links. For time intervals 1 through 6, this average is computed during time 5:00-5:10, 5:10-5:20, 5:20-5:30, 5:30-5:40, 5:40-5:50 and 5:50-6:00, respectively. This figure illustrates the impact of the signal plans on local (link-level) performance.

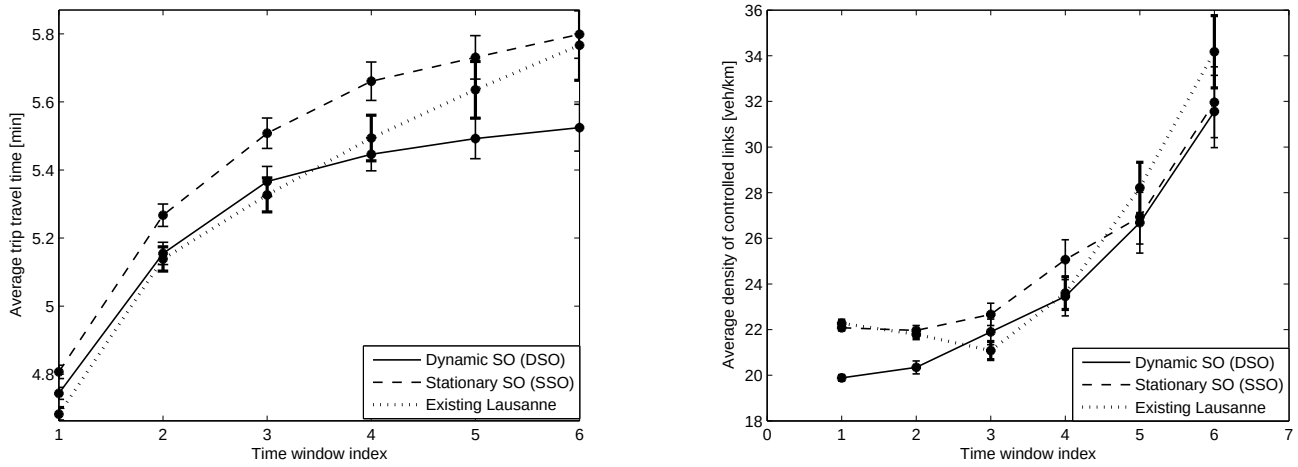

(a) Time-dependent average trip travel time

(b) Time-dependent average link density of the signal controlled links

Figure 8 Time-dependent congestion metrics of the best DSO, the best SSO and the Lausanne plans

Figure 8(a) indicates that as congestion increases, so does the difference in performance between the DSO plan and the 2 other plans. Figure 8(b) indicates that the main difference between the DSO plan and the 2 other plans is that the DSO plan leads to significantly lower levels of congestion at the start of the peak-period. As a consequence, it delays the onset and the propagation of congestion. This is observed in Figure 8(a), where the travel times at 6pm under the DSO plan are those observed under the Lausanne plan around 5:30pm, and under the SSO plan around 5:40 pm. Figures 8(a) and 8(b) indicate that as congestion increases, so does the variance of the estimators. This increased variance illustrates one of the challenges of performing SO for congested scenarios, where the objective function estimators tend to have high variance.

4.4. Comparison with a signal plan derived by commercial signal control software

We compare the performance of the best DSO signal plan with that of a signal plan derived with the signal control software Synchro, which is a mainstream, commercial and popular signal control software (Trafficware (2011)). It is widely used across the United States. Major cities, such as New York, rely on it to design their signal plans (NYCDOT 2012). For details on Synchro's green split optimization technique, we refer the reader to Chapter 14 of Trafficware (2011). Synchro is based on a macroscopic, deterministic and local traffic model. We give Synchro the same input data (e.g., network and traffic data) as for the DSO method. The details on the Synchro input configuration used are given in Osorio and Chong (Section 5.3, 2015). As before, the best DSO signal plan is that with the lowest average trip travel time among the 12 plans derived by DSO (i.e., left-most cdf curve of Figure 3(b)).

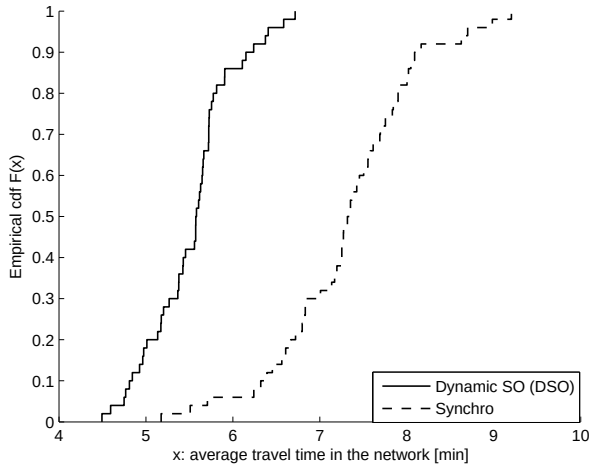

(a) Comparison of the expected trip travel time of the best DSO signal plan and the signal plan derived by Synchro

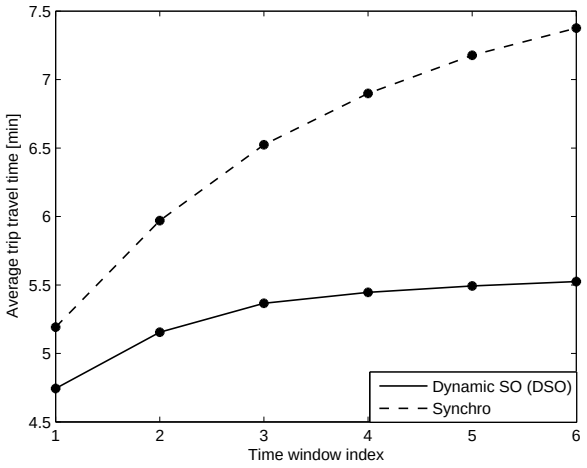

(b) Comparison of the time-dependent expected trip travel time of the best DSO signal plan and the signal plan derived by Synchro

Figure 9 Comparison of the performance metric of the best DSO signal plan and the signal plan derived by Synchro

To evaluate the performance of the Synchro and the DSO signal plans, we proceed as in Section 4.3. Figure 9(a) displays the cdf of the average trip travel time of the DSO signal plan (solid curve) and of the Synchro plan (dashed curve). The DSO plan yields a significant improvement in the average trip travel times. The average objective function value, among the 50 simulation replications, is 5.5 minutes for the DSO plan and 7.3 minutes for the Synchro plan. The DSO plan yields a 25% reduction in the trip travel times compared to the Synchro plan.

Figure 9(b) evaluates the performance of the plans as a function of time. This figure considers the same performance metrics as the plots of Figure 5, i.e., the x-axis considers the 5pm-6pm period discretized in 10 minute time increments, and the y-axis displays the average trip travel time. As a result, the best DSO plan outperforms the Synchro plan for all the six time intervals. This figure indicates that, as congestion increases, the DSO plan mitigates the increase in the travel times, while the Synchro plan leads to higher travel times.

5. Conclusions

This paper proposes a novel metamodel method that addresses large-scale simulation-based urban transportation optimization problems with time-dependent decision variables. The proposed metamodel embeds a tractable transient network model that accounts for the time variations of traffic flow and the temporal propagation of congestion in the underlying road network. The transient network model is formulated based on transient queueing theory. The proposed transient metamodel method is a computationally efficient

technique that identifies good solutions (e.g., signal plans) under tight computational budget.

We evaluate the performance of this approach by addressing a large-scale network-wide time-dependent signal control problem for the Swiss city of Lausanne. This problem considers a congested network (evening peak period demand) with an intricate topology. We compare the performance of the proposed dynamic metamodel SO method with that of a stationary metamodel SO method proposed by Osorio and Chong (2015). The dynamic metamodel SO method identifies signal plans that outperform both the initial signal plans, and most often, the signal plans derived by the stationary metamodel SO method. The analysis of this paper also illustrates that the best DSO plan outperforms an existing signal plan for the city of Lausanne, as well as a plan derived by Synchro.

This paper allows practitioners to use a computationally efficient SO method to address a variety of dynamic large-scale transportation problems. In this paper, the analytical transient network model is used to approximate the simulation-based objective function. Of current interest is the study of the use of this model to enhance other algorithmic steps, such as sampling strategies and ranking and selection strategies to statistically compare the performance of multiple points. As part of ongoing research, we are extending the use of the proposed transient metamodel SO method to address traffic-responsive simulation-based optimization problems.

This paper considers SO problems where the constraints are available in analytical, rather than simulation-based form. Problems with simulation-based (i.e., stochastic) constraints require evaluating the feasibility of a point via simulation. The feasibility of a point cannot be guaranteed. It can be tested statistically but at the computational cost of obtaining an accurate estimate of the simulation-based constraints. In other words, numerous simulation replications need to be run in order to test for feasibility. For this reason, SO problems with simulation-based constraints can be computationally more challenging to address. In transportation, examples of stochastic constraints would be, for instance, bounds on link or network performance metrics (e.g., travel times, emissions, energy consumption). Efficient algorithms for such problems are needed. The metamodel ideas of this paper could be used to formulate computationally efficient algorithms for SO problems with stochastic constraints. In other words, problem-specific analytical metamodels of the stochastic constraints can be formulated.

Discrete SO problems are another family of problems, where these metamodel ideas could prove beneficial. There is a lack of efficient methods for such problems, yet many network design problems are naturally formulated as discrete problems. As part of ongoing work in bike-sharing and car-sharing problems, we are exploring ideas in this area.

Acknowledgements

This material is based upon work partly supported by the National Science Foundation under Grant No. 1351512. Any opinions, findings, and conclusions or recommendations expressed in this material are those of the authors and do not necessarily reflect the views of the National Science Foundation.

References

Aboudolas, K., M. Papageorgiou, E. Kosmatopoulos. 2007. Control and optimization methods for traffic signal control in large-scale congested urban road networks. *American Control Conference*. 3132–3138.

Aboudolas, K., M. Papageorgiou, A. Kouvelas, E. Kosmatopoulos. 2010. A rolling-horizon quadratic-programming approach to the signal control problem in large-scale congested urban road networks. *Transportation Research Part C: Emerging Technologies* **18**(5) 680 – 694.

Almeder, C, M Preusser, R Hartl. 2009. Simulation and optimization of supply chains: alternative or complementary approaches? *OR spectrum* **31**(1) 95–119.

Balakrishna, R. 2006. Off-line calibration of dynamic traffic assignment models. Ph.D. thesis, Massachusetts Institute of Technology.

Barton, R, M Meckesheimer. 2006. Metamodel-based simulation optimization. S G Henderson, B L Nelson, eds., *Handbooks in operations research and management science: Simulation*, vol. 13, chap. 18. Elsevier, Amsterdam, 535–574.

Ben-Akiva, M, D Cuneo, M Hasan, M Jha, Q Yang. 2003. Evaluation of freeway control using a microscopic simulation laboratory. *Transportation research Part C: emerging technologies* **11**(1) 29–50.

Bocharov, P, C D'Apice, A Pechinkin, S Salerno. 2004. *Queueing theory*, chap. 3. Modern Probability and Statistics, Brill Academic Publishers, Zeist, The Netherlands, 96–98.

Branke, J, P Goldate, H Prothmann. 2007. Actuated traffic signal optimization using evolutionary algorithms. *Proceedings of the 6th European Congress and Exhibition on Intelligent Transport Systems and Services*.

Bullock, D, B Johnson, R Wells, M Kyte, Z Li. 2004. Hardware-in-the-loop simulation. *Transportation Research Part C* **12**(1) 73 – 89.

Chen, X, C Osorio, M Marsico, M Talas, J Gao, S Zhang. 2015. Simulation-based adaptive traffic signal control algorithm. *Proceedings of the Transportation Research Board Annual Meeting*. Washington DC, USA.

Cohen, J W. 1982. *The single server queue*, chap. III.6. Applied mathematics and mechanics, North-Holland Publishing Company, The Netherlands.

Coleman, T F, Y Li. 1994. On the convergence of reflective Newton methods for large-scale nonlinear minimization subject to bounds. *Mathematical Programming* **67**(2) 189–224.

Coleman, T F, Y Li. 1996. An interior, trust region approach for nonlinear minimization subject to bounds. *SIAM Journal on Optimization* **6** 418–445.

Conn, A R, K Scheinberg, L N Vicente. 2009. *Introduction to derivative-free optimization*. MPS/SIAM Series on Optimization, Society for Industrial and Applied Mathematics and Mathematical Programming Society, Philadelphia, PA, USA.

Dinopoulou, V, C Diakaki, M Papageorgiou. 2006. Applications of the urban traffic control strategy tuc. *European Journal of Operational Research* **175**(3) 1652–1665.

Dumont, A, E Bert. 2006. Simulation de l'agglomération Lausannoise SIMLO. Technical report, Laboratoire des voies de circulation, ENAC, Ecole Polytechnique Fédérale de Lausanne.

Gartner, N, D Hou. 1992. Comparative evaluation of alternative traffic control strategies. *Transportation Research Record* (1360).

Hale, D. 2005. Traffic network study tool TRANSYT-7F. Technical report, McTrans Center in the University of Florida, Gainesville, Florida.

Hasan, M, M Jha, M Ben-Akiva. 2002. Evaluation of ramp control algorithms using microscopic traffic simulation. *Transportation Research Part C* **10**(3) 229–256.

Heidemann, D. 2001. A queueing theory model of nonstationary traffic flow. *Transportation Science* **35**(4) 405–412.

Joshi, S, A Rathi, J Tew. 1995. An improved response surface methodology algorithm with an application to traffic signal optimization for urban networks. C Alexopoulos, K Kang, W R Lilegdon, D Goldsman, eds., *Proceedings of the Winter Simulation Conference*. Arlington, VA, USA, 1104–1109.

Jung, J Y, G Blau, J F Pekny, G V Reklaitis, D Eversdyk. 2004. A simulation based optimization approach to supply chain management under demand uncertainty. *Computers and Chemical Engineering* **28** 2087–2106.

Kolda, T, R Lewis, V Torczon. 2003. Optimization by direct search: New perspectives on some classical and modern methods. *SIAM Review* **45**(3) 385–482.

Kwak, J, B Park, J Lee. 2012. Evaluating the impacts of urban corridor traffic signal optimization on vehicle emissions and fuel consumption. *Transportation Planning and Technology* **35**(2) 145–160.

Legato, P, R M Mazza, R Trunfio. 2008. Simulation-based optimization for the quay crane scheduling problem. SJ Mason, R Hill, L Moench, O Rose, eds., *Proceedings of the Winter Simulation Conference*. 2717–2725.

Li, P, M Abbas, R Pasupathy, L Head. 2010. Simulation-based optimization of maximum green setting under retrospective approximation framework. *Transportation Research Record* **2192** 1–10.

Lin, S. 2011. Efficient model predictive control for large-scale urban traffic networks. Ph.D. thesis, Delft University of Technology.

Little, J. 1961. A proof for the queuing formula: L= λ W. *Operations Research* **9**(3) 383–387.

Morse, P. 1958. *Queues, inventories and maintenance; the analysis of operational systems with variable demand and supply*. Wiley, New York, USA.

NYCDOT. 2012. Downtown Flushing,mobility and safety improvemnt project. Technical report, New York City Department of Transportation.

Odoni, A, E Roth. 1983. An empirical investigation of the transient behavior of stationary queueing systems. *Operations Research* **31**(3) 432–455.

Osorio, C. 2010. Mitigating network congestion: analytical models, optimization methods and their applications. Ph.D. thesis, Ecole Polytechnique Fédérale de Lausanne.

Osorio, C, M Bierlaire. 2013. A simulation-based optimization framework for urban transportation problems. *Operations Research* **61**(6) 1333–1345.

Osorio, C, X Chen, M Marsico, M Talas, J Gao, S Zhang. 2014. Reducing gridlock probabilities via simulation-based signal control. *Proceedings of the International Symposium on Transport Simulation (ISTS)*. Under review for journal publication, version available at: http://web.mit.edu/osorioc/www/papers/osoChenNYCDOTOfflineSO.pdf .

Osorio, C, X Chen, B F Santos. 2016. Simulation-based travel time reliable signal control. Submitted. Available at: http://web.mit.edu/osorioc/www/papers/osoCheSanReliableSO.pdf .

Osorio, C, L Chong. 2015. A computationally efficient simulation-based optimization algorithm for large-scale urban transportation problems. *Transportation Science* **49**(3) 623–636.

Osorio, C, G Flötteröd. 2014. Capturing dependency among link boundaries in a stochastic dynamic network loading model. *Transportation Science* **49**(2) 420–431.

Osorio, C, G Flötteröd, M Bierlaire. 2011. Dynamic network loading: a stochastic differentiable model that derives link state distributions. *Transportation Research Part B* **45**(9) 1410–1423.

Osorio, C, G Flötteröd, C Zhang. 2015. A metamodel simulation-based optimization approach for the efficient calibration of stochastic traffic simulators. *Transportation Research Procedia* **6** 213–223. Papers selected for the 4th International Symposium of Transport Simulation (ISTS'14).

Osorio, C, K Nanduri. 2015a. Energy-efficient urban traffic management: a microscopic simulation-based approach. *Transportation Science* **49**(3) 637–651.

Osorio, C, K Nanduri. 2015b. Urban transportation emissions mitigation: Coupling high-resolution vehicular emissions and traffic models for traffic signal optimization. *Transportation Research Part B: Methodological* **81** 520–538.

Osorio, C, K Selvam. 2015. Simulation-based optimization: achieving computational efficiency through the use of multiple simulators. *Transportation Science* Forthcoming. Available at: http://web.mit.edu/osorioc/www/papers/osoSelMultiModel.pdf .

Park, B, I Yun, K Ahn. 2009. Stochastic optimization for sustainable traffic signal control. *International Journal of Sustainable Transportation* **3**(4) 263–284.

Peterson, M D, D J Bertsimas, A R Odoni. 1995. Decomposition algorithms for analyzing transient phenomena in multiclass queueing networks in air transportation. *Operations Research* **43**(6) 995–1011.

Rathi, A K, E B Lieberman. 1989. Effectiveness of traffic restraint for a congested urban network: a simulation study. *Transportation Research Record* **1232** 95–102.

Schwartz, J D, W Wang, D E Rivera. 2006. Simulation-based optimization of process control policies for inventory management in supply chains. *Automatica* **42** 1311–1320.

Stafford, R. 2006. *The Theory Behind the 'randfixedsum' Function*. Http://www.mathworks.com/matlabcentral/fileexchange/9700 .

Stallard, C, L Owen. 1998. Evaluating adaptive signal control using CORSIM. D Medeiros, E Watson, J Carson, M Manivannan, eds., *Proceedings of the 1998 Winter Simulation Conference*. Washington, D.C., USA, 1147–1154.

Stevanovic, A, J Stevanovic, K Zhang, S Batterman. 2009. Optimizing traffic control to reduce fuel consumption and vehicular emissions. integrated approach with VISSIM, CMEM, and VISGAOST. *Transportation Research Record* **2128** 105–113.

Stevanovic, J, A Stevanovic, P T Martin, T Bauer. 2008. Stochastic optimization of traffic control and transit priority settings in VISSIM. *Transportation Research Part C* **16**(3) 332 – 349.

Trafficware. 2011. *Synchro Studio 8 User Guide*. Trafficware, Sugar Land, TX.

TSS. 2011. *AIMSUN 6.1 Microsimulator Users Manual*. Transport Simulation Systems.

VSS. 1992. *Norme Suisse SN 640837 Installations de feux de circulation; temps transitoires et temps minimaux*. Union des professionnels suisses de la route, VSS, Zurich.

Yun, I, B Park. 2006. Application of stochastic optimization method for an urban corridor. L F Perrone, F P Wieland, J Liu, B G Lawson, D M Nicol, R M Fujimoto, eds., *Proceedings of the Winter Simulation Conference*. Monterey, CA, USA, 1493–1499.

Appendix A: Metamodels for transportation problems

In our past work, we have developed efficient SO algorithms for various transportation problems with case studies of Lausanne (Switzerland), Manhattan (NYC, USA) and Berlin (Germany). We summarize here the main insights obtained from past work. The formulation presented in this paper is motivated by these insights. Table 4 summarizes the main features of the methods and case studies used for signal control problems. The last row represents the present paper. The second

Table 4 Summary of metamodel SO methods for signal control problems

	Model		Outperforms			Number of			Metamodel of
	Stat.	Trans.	Random	Field	Synchro	Roads	Inter.	Dec. var.	
Osorio and Bierlaire (2013)	✓		✓	✓		48	15	51	Trip travel time
Osorio and Nanduri (2015a)	✓		✓			47	15	51	Fuel consumption and trip travel time
Osorio and Nanduri (2015b)	✓		✓	✓		47	15	51	Pollutant emissions and trip travel time
Osorio et al. (2014)	✓		✓	✓		134	32	64	Queue-lengths
Osorio et al. (2016)	✓		✓			603	231	99	Link travel time variance and expectation
Osorio and Chong (2015)	✓		✓		✓	603	231	99	Trip travel time
Chong and Osorio		✓	✓	✓	✓	603	231	198	Trip travel time

and third columns indicate whether the SO method is designed for time-independent or time-dependent problems. More specifically, these methods embed information from analytical traffic models. Columns 2 and 3 indicate whether the analytical models are stationary or transient, respectively. Columns 4-6 indicate whether the case studies have benchmarked the derived signal plans versus signal plans that are: randomly drawn, prevailing in the field or derived from the commercial signal control software Synchro. Columns 7-9 indicate the number of roads, of intersections and of decision variables of the case studies. For papers that include multiple case studies, the table indicates the largest-scale case study. The last column indicates the objective function.

Column 2 indicates that all past work has formulated metamodels with stationary traffic models. The present paper is the first to formulate a metamodel with a transient (i.e., time-dependent) traffic model. This table indicates that formulations for a variety of objective functions have been proposed and successfully used for problems that are considered large-scale for both signal control and for SO.

Recall that in a metamodel framework, the objective function needs to be approximated analytically by the metamodel. For a specific objective function, the key to designing a computationally efficient SO algorithm lies in the formulation of an analytical traffic model that is both: (i) a good approximation of the unknown objective function, and (ii) is sufficiently tractable such that Problem (6)-(8) can be solved efficiently. Column 10 of the table indicates that we have designed algorithms for objective functions that are intricate to approximate analytically (e.g., vehicular emissions, fuel consumption, travel time variability).

All these case studies include analysis with tight computational budgets, where the simulation budget ranges from 50 to 150. Even for such tight budgets, the signal plans identified by the metamodel methods outperform a variety of signal plans: (i) randomly drawn plans, (ii) plans prevailing in the field, and (iii) plans derived by mainstream widely used commercial software. The results of these various case studies consistently indicate that the ability of these SO methods to identify good solutions under tight budgets is due to the combination of simulation observations with analytical traffic model information.

More specifically, the papers tabulated in Table 4 (excluding Osorio et al. (2014)) have benchmarked the metamodel of Equation (5) with a metamodel that does not include information from the analytical traffic model (i.e., $m = \phi$ in (5)). All case studies have shown that by embeding information from analytical traffic models, the following properties are achieved: (i) solutions with

better performance are identified, (ii) good quality solutions are identified within significantly fewer simulation runs, and (iii) the algorithm becomes robust to the quality of the initial points. Note that a metamodel approach with $m = \phi$ (i.e., with a local quadratic general-purpose metamodel) is a traditional SO approach. It corresponds to an iterative response-surface methodology, which is broadly and commonly used in the literature and is often not referred to as a metamodel technique. For lower-dimensional problems with larger computational budgets (i.e., easier problems to solve), the traditional approach and the metamodel with analytical traffic information identify solutions with similar performance (see Osorio and Bierlaire (2013), for problems with: (i) 2 controlled intersections, a decision vector of dimension 13 and a buget of 750, and (ii) 9 controlled intersections, a decision vector of dimension 51 and a budget of 3000).

Recent work has investigated what type of structural information provided by the analytical traffic model is key to identifying signal plans that perform well for networks with high levels of congestion and intricate traffic patterns (Osorio et al. 2014). The latter work considered a Manhattan case study. It indicates that providing the algorithm with an analytical description of between-link interactions or dependencies is critical to identifying signal plans that can contribute to mitigate congestion. In particular, the algorithms are particularly efficient when they are provided with an analytical description of the occurrence and the impact of vehicular spillbacks. The analytical traffic model formulated in this paper builds upon these insights. It proposes a time-dependent description of spillback probabilities, and it accounts for the impact of spillbacks on the underlying link's flow capacity.

These metamodel ideas have been recently used to efficiently address two other classes of optimization problems. First, metamodels have been formulated for an offline demand calibration problem for the metropolitan area of Berlin (Osorio et al. 2015). The formulated analytical traffic model is shown to provide a highly accurate approximation of the unknown simulation-based objective function. The time-dependent model formulated in the present paper can be used to extend the ideas in Osorio et al. (2015) for online calibration problems. This calibration work also illustrates the use of these metamodel ideas for problems where the decision variables are demand, rather than supply, variables. In particular, in that work the decision variables are coefficients of a route choice model. Second, metamodels have been formulated to design multi-model SO algorithms, where multiple simulators with different computational runtime costs are jointly used (Osorio and Selvam 2015).

This past work highlights that these metamodel ideas have been successfully used to address problems with intricate objective functions, intricate traffic patterns (e.g., Manhattan), and very different demand-supply interactions. This encourages us to design algorithms for real-time problems. The time-dependent formulation proposed in this paper is a first-step towards this goal.

Appendix B: Trust region subproblem

To formulate the trust region (TR) subproblem that is solved at each iteration k of the SO algorithm, we use the following notation.

x	vector of decision variables;
x_ℓ	vector of green splits for time interval ℓ;
$x_\ell(j)$	green split of signal phase j for time interval ℓ;
x_{LB}	vector of lower bounds for green splits;
x_k	current iterate at iteration k;
$\mu_{d,\ell}$	service rate of lane d for time interval ℓ;
y	vector of endogenous variables;
q	vector of exdogenous parameters;
β_k	vector of metamodel parameters at iteration k;
Δk	trust region radius at iteration k;
b_i	ratio of available cycle time to total cycle time for intersection i;
e_d	ratio of fixed green time to cycle time of signalized lane d;
s	satuation flow rate;
$\mathscr{P}_D(d)$	set of endogenous phase indices of lane d;
$\mathscr{I}$	set of intersection indices;
$\mathscr{P}_I(i)$	set of endogenous signal phase indices of intersection i.

The TR subproblem is formulated as follows.

$$\min_x \; m_k(x, y; q, \beta_k) \tag{32}$$

subject to

$$\sum_{j \in \mathscr{P}_I(i)} x_\ell(j) = b_i \;\; \forall i \in \mathscr{I}, \ell \in \mathcal{L} \tag{33}$$

$$h(x, y; q) = 0 \tag{34}$$

$$\mu_{d,\ell} - \sum_{j \in \mathscr{P}_D(d)} x_\ell(j) s = e_d s, \;\; \forall d \in \mathcal{D}, \ell \in \mathcal{L} \tag{35}$$

$$\|x - x_k\|_2 \leq \Delta_k \tag{36}$$

$$y \geq 0 \tag{37}$$

$$x_\ell \geq x_{LB}, \forall \ell \in \mathcal{L}. \tag{38}$$

The objective function is the metamodel $m_k(x, y; \beta_k, q)$. Equations (33) and (38) are the signal control constraints, they correspond to Equations (16) and (17). The function h of Equation (34) represents the transient network model. It represents Equations (10a)-(10c). Equation (35) associates the green splits of a phase with the flow capacity of the underlying lanes (i.e., the service rate of the queues). Constraint (36) is the trust region constraint, where Δ_k is the trust region radius. The endogenous variables of the queueing model are subject to positivity constraints (Equation (37)). Thus, the TR subproblem consists of a nonlinear objective function subject to nonlinear equalities, linear equalities, a nonlinear inequality and bound constraints.

The TR subproblem is solved with the Matlab routine for constrained nonlinear problems, *fmincon*, and its interior point programming method (Coleman and Li 1996, 1994). We set the tolerance for relative change in the objective function to 10^{-3} and the tolerance for the maximum constraint violation to 10^{-3}. For further details on the TR subproblem formulation and its implementation, see Osorio and Chong (2015).

Appendix C: Derivative of the objective function

This appendix serves to illustrate how the analytical expression for the objective and constraint functions of Problem (15)-(17) are derived. The example we provide is for the derivative of the objective function (denoted $f_{A,\ell}$ in Equation (18)) with regards to the variable $\hat{\rho}_{i,\ell}$. The analytical form of any other derivative with respect to any of the endogenous variables can be derived following the same logic.

By definition, we have:

$$f_{A,\ell} = \frac{\sum_i E_\ell[N_i]}{\frac{1}{t_\ell - t_{\ell+1}} \int_{t_\ell}^{t_{\ell+1}} \sum_i \gamma_i (1 - P_\ell(N_i = k_i, t)) dt}. \tag{39}$$

Let C denote the numerator and D denote the denominator. Following the quotient rule, we obtain:

$$\frac{\partial f_{A,\ell}}{\partial \hat{\rho}_{i,\ell}} = \frac{\frac{\partial C}{\partial \hat{\rho}_{i,\ell}}}{D} - \frac{\frac{\partial D}{\partial \hat{\rho}_{i,\ell}} C}{D^2}. \tag{40}$$

We first derive the analytical expression for $\frac{\partial C}{\partial \hat{\rho}_{i,\ell}}$, then we derive that of $\frac{\partial D}{\partial \hat{\rho}_{i,\ell}}$.

Using the chain rule, we have:

$$\frac{\partial C}{\partial \hat{\rho}_{i,\ell}} = \frac{\partial E_\ell[N_i]}{\partial \rho_{i,\ell}} \frac{\partial \rho_{i,\ell}}{\partial \hat{\rho}_{i,\ell}}. \tag{41}$$

The analytical form of $E_\ell[N_i]$ and $\rho_{i,l}$ are given in Equations (20) and (21), respectively.

Equation (20) can be rewritten as:

$$E_\ell[N_i] = \frac{\rho_{i,\ell}}{1 - \rho_{i,\ell}} - \frac{(k_i + 1) {\rho_{i,\ell}}^{k_i+1}}{1 - {\rho_{i,\ell}}^{k_i+1}}, \tag{42}$$

and its derivate is given by:

$$\frac{\partial E_\ell[N_i]}{\partial \rho_{i,\ell}} = \frac{1}{(1 - \rho_{i,\ell})^2} - \frac{(k_i + 1)^2 \rho^{k_i}}{(1 - \rho_{i,\ell}^{k_i+1})^2}. \tag{43}$$

Equation (21) can be rewritten as:

$$\rho_{i,\ell} = (t_{\ell+1} - t_\ell) \frac{\hat{\rho}_{i,\ell}}{A}, \tag{44}$$

where A is defined by Equation (22). This leads to:

$$\frac{\partial \rho_{i,\ell}}{\partial \hat{\rho}_{i,\ell}} = (t_{\ell+1} - t_\ell)(\frac{1}{A} - \frac{\hat{\rho}_{i,\ell}}{A^2} \frac{\partial A}{\partial \hat{\rho}_{i,\ell}}). \tag{45}$$

In order to derive an expression for $\frac{\partial A}{\partial \hat{\rho}_{i,\ell}}$, we use the analytical expresion of A given by Equation (25), this leads to:

$$\begin{aligned}
\frac{\partial A}{\partial \hat{\rho}_{i,\ell}} &= \frac{\partial \tau_{i,\ell}}{\partial \hat{\rho}_{i,\ell}} \left[(P_\ell(N_i = k_i, t_\ell) - P_\ell(N_i = k_i))(e^{-\frac{t_{\ell+1}}{\tau_{i,\ell}}} - e^{-\frac{t_\ell}{\tau_{i,\ell}}}) \right] + \dots \\
&\cdots + \tau_{i,\ell}(P_\ell(N_i = k_i, t_\ell) - P_\ell(N_i = k_i)) \left(\frac{\partial e^{-\frac{t_{\ell+1}}{\tau_{i,\ell}}}}{\partial \hat{\rho}_{i,\ell}} - \frac{\partial e^{-\frac{t_\ell}{\tau_{i,\ell}}}}{\partial \hat{\rho}_{i,\ell}} \right) \qquad (46) \\
&= \frac{\partial \tau_{i,\ell}}{\partial \hat{\rho}_{i,\ell}} \left[(P_\ell(N_i = k_i, t_\ell) - P_\ell(N_i = k_i))(e^{-\frac{t_{\ell+1}}{\tau_{i,\ell}}} - e^{-\frac{t_\ell}{\tau_{i,\ell}}}) \right] + \dots \\
&\cdots + (P_\ell(N_i = k_i, t_\ell) - P_\ell(N_i = k_i)) \left(\frac{t_{\ell+1}}{\tau_{i,\ell}} e^{-\frac{t_{\ell+1}}{\tau_{i,\ell}}} \frac{\partial \tau_{i,\ell}}{\partial \hat{\rho}_{i,\ell}} - \frac{t_\ell}{\tau_{i,\ell}} e^{-\frac{t_\ell}{\tau_{i,\ell}}} \frac{\partial \tau_{i,\ell}}{\partial \hat{\rho}_{i,\ell}} \right). \qquad (47)
\end{aligned}$$

Equation (46) is obtained by observing that the derivative of $(t_{\ell+1} - t_\ell)(1 - P_\ell(N_i = k_i))$ with regards to $\hat{\rho}_{i,\ell}$ is zero. This is because the terms $t_{\ell+1}$ and t_ℓ are constant, and because $\frac{\partial P_\ell(N_i = k_i)}{\partial \hat{\rho}_{i,\ell}} = 0$,

since both $P_\ell(N_i = k_i)$ and $\hat{\rho}_{i,\ell}$ are both endogenous variables. And because $P_\ell(N_i = k_i, t_\ell)$ is the initial spillback probably at interval ℓ and does not depend on $\hat{\rho}_{i,\ell}$, $\frac{\partial P_\ell(N_i=k_i,t_\ell)}{\partial \hat{\rho}_{i,\ell}} = 0$.

In order to derive $\frac{\partial \tau_{i,\ell}}{\partial \hat{\rho}_{i,\ell}}$, let us recall that $\tau_{i,\ell}$ is defined in Equation (14b) by:

$$\tau_{i,\ell} = \frac{ck_i}{\hat{\lambda}_{i,\ell}} \frac{\hat{\rho}_{i,\ell}}{(1-\sqrt{\hat{\rho}_{i,\ell}})^2}. \tag{48}$$

Therefore,

$$\frac{\partial \tau_{i,\ell}}{\partial \hat{\rho_{i,\ell}}} = \frac{ck_i}{\hat{\lambda}_{i,\ell}} \partial \left(\frac{\hat{\rho}_{i,\ell}}{(1-\sqrt{\hat{\rho}_{i,\ell}})^2}\right) / \partial \hat{\rho}_{i,\ell} \tag{49}$$

$$= \frac{ck_i}{\hat{\lambda}_{i,\ell}} \left(\frac{1}{(1-\sqrt{\hat{\rho}_{i,\ell}})^2} - \frac{\hat{\rho}_{i,l} \frac{\partial((1-\sqrt{\hat{\rho}_{i,\ell}})^2)}{\partial \hat{\rho}_{i,\ell}}}{(1-\sqrt{\hat{\rho}_{i,\ell}})^4} \right) \tag{50}$$

$$= \frac{ck_i}{\hat{\lambda}_{i,\ell}} \left(\frac{1}{(1-\sqrt{\hat{\rho}_{i,\ell}})^2} + \frac{\sqrt{\hat{\rho}_{i,\ell}}}{(1-\sqrt{\hat{\rho}_{i,\ell}})^3} \right). \tag{51}$$

Note that Equation (49) is derived by observing that $\frac{\partial \hat{\lambda}_{i,\ell}}{\partial \hat{\rho}_{i,\ell}} = 0$, since both variables are endogenous.

Combining Equations (41), (43), (45), (47) and (51), we obtain the analytical derivative of the numerator of the objective function, $\frac{\partial C}{\partial \hat{\rho}_{i,\ell}}$.

In order to derive the derivative of the denominator D, note that it can be expressed as the following function of A:

$$D = \frac{1}{t_\ell - t_{\ell+1}} \sum_i \gamma_i A. \tag{52}$$

Thus,

$$\frac{\partial D}{\partial \hat{\rho}_{i,\ell}} = \frac{\gamma_i}{(t_{\ell+1} - t_\ell)} \frac{\partial A}{\partial \hat{\rho}_{i,\ell}}. \tag{53}$$

The expression for $\frac{\partial A}{\partial \hat{\rho}_{i,\ell}}$ is given by Equation (47).